TABLE 1. Characteristics of Enrolled Patients

	PpPD (n = 64)	PrPD (n = 66)	P
Age, yrs	68 ± 9	67 ± 9	0.5776
Gender (male/female)	33/31	38/28	0.6084
Diabetes (yes/no)	18/46	19/47	0.9999
Preoperative biliary drainage (yes/no)	34/33	26/40	0.2532
Diabetes (yes/no)	18/46	19/47	0.9999
Serum hemoglobin, g/dL*	13.0 ± 1.5	12.5 ± 1.3	0.2184
Serum creatinine, mg/dL†	0.68 ± 0.2	0.72 ± 0.2	0.1903
Serum total bilirubin, mg/dL‡	3.8 ± 4.0	4.0 ± 6.0	0.7965
Serum amylase, IU/L§	124 ± 134	111 ± 104	0.5232
Benign tumors/malignant tumors	12/52	14/52	0.8953
Pancreatic adenocarcinoma	17	23	
Bile duct carcinoma	18	15	
Ampullary adenocarcinoma	6	3	
Duodenal adenocarcinoma	0	1	
Intraductal papillary neoplasms	15	15	
Pancreatic endocrine tumor	1	2	
Tumor forming pancreatitis	3	5	
Other disease	4	2	
Operative time, min	342 ± 71	358 ± 84	0.2631
Intraoperative bleeding, mL	820 ± 987	902 ± 1075	0.6527
Red blood cell transfusion, units	1.1 ± 3.0	1.9 ± 5.0	0.2400
Lymph node dissection (D1/D2)	9/55	9/57	0.9999
Portal vein resection (yes/no)	5/59	10/56	0.3007

*Normal range of hemoglobin: 12–17.5 g/dL.
†Normal range of creatinine: 0.53–1.02 mg/dL.
‡Normal range of total bilirubin: 0.2–1.2 mg/dL.
§Normal range of amylase: 15–150 IU/L.

n = 12; PrPD: n = 14). Background data and perioperative status were similar in the 2 groups.

Incidence of DGE and Postoperative Course Associated With DGE

The overall incidence of DGE in this RCT was 10.8% (14 of the 130 patients); the overall incidence of DGE was 4.5% in PrPD and 17.2% in PpPD, a significant difference ($P = 0.0244$). Delayed gastric emptying was classified into 3 categories by ISGPS.[30] The proposed clinical grading of 11 patients with DGE in PpPD are grade A (n = 6), grade B (n = 5), and grade C (n = 0). In PrPD, 1 patient in each grade classification reported DGE. The 2 groups did not differ significantly in management of the nasogastric catheter, start of solid foods, and postoperative length of hospital stay (Table 2).

Time of passage from esophagogastric junction to gastrojejunostomy or duodenojejunostomy by postoperative upper gastrointestinal gastrografin series on postoperative day 7 was significantly delayed in PpPD compared with PrPD (27.2 ± 31.3 s versus 10.1 ± 9.0 s, $P < 0.0001$). The results of the time of peak $^{13}CO_2$ content are shown in Table 2. The time of peak $^{13}CO_2$ content at 1, 3, and 6 months after surgery in PpPD was significantly delayed compared with PrPD (34.3 ± 24.6 minutes versus 18.7 ± 11.8 minutes, 26.5 ± 21.1 minutes versus 17.3 ± 11.7 minutes, and 26.7 ± 18.8 minutes versus 17.4 ± 13.2 minutes, respectively). Thus, the gastric emptying of ^{13}C-acetate breath test or postoperative upper gastrointestinal gastrografin series was significantly delayed in patients in the PpPD group compared with those undergoing PrPD (Table 3).

TABLE 2. Delayed Gastric Emptying and Postoperative Course

	PpPD (n = 64)	PrPD (n = 66)	P
Delayed gastric emptying*	11 (17.2%)	3 (4.5%)	0.0244
Grade A	6 (9.4%)	1 (1.5%)	
Grade B	5 (7.8%)	1 (1.5%)	
Grade C	0 (0%)	1 (1.5%)	
Removal of nasogastric catheter, d	0.6 ± 0.9	0.6 ± 1.0	0.9410
Reinsertion of nasogastric catheter	8 (12.5%)	2 (3.0%)	0.0527
Start of solid diet, d	6.3 ± 3.7	5.6 ± 3.3	0.1138
Postoperative hospital stay, d	24.1 ± 14.8	24.3 ± 15.5	0.9305

*Delayed gastric emptying is defined according to the International Study Group of Pancreatic Surgeons.

TABLE 3. Results of Gastric Emptying Assessed by ^{13}C-Acetate Breath Test

	PpPD (n = 64)	PrPD (n = 66)	P
Postoperative upper gastrointestinal gastrografin series, s*	27.2 ± 31.3	10.1 ± 9.0	0.0001
^{13}C-acetate breath test, min†			
1 mo after surgery	34.0 ± 24.1	18.7 ± 29.7	<0.0001
3 mo after surgery	26.5 ± 21.1	17.3 ± 11.7	0.0136
6 mo after surgery	26.7 ± 18.8	17.4 ± 13.2	0.0197

*Time for the passage of gastrografin from esophagogastric junction to gastrojejunostomy or duodenojejunostomy was measured on postoperative day 7.
†Gastric emptying was evaluated by the time of peak $^{13}CO_2$ content in ^{13}C-acetate breath test at 1, 3, and 6 months after surgery.

Postoperative Complications

Table 4 shows the other postoperative complications in the PpPD and PrPD groups. The groups did not differ significantly in the incidence of other postoperative complications, specifically, clinically relevant pancreatic fistula, intra-abdominal abscess, and intra-abdominal hemorrhage. The overall rate of pancreatic fistula in this RCT was 29.2% (38 of 130 patients). Moreover, pancreatic fistula was classified into 3 categories by ISGPF[31]: grade A in 22 of the 130 patients (16.9%), grade B in 12 patients (9.2%), and grade C in 4 patients (3.1%). Ultrasonography-guided percutaneous drainage was required for intra-abdominal abscess in 14 (10.7%) of the 130 patients. Moreover, there was no significant difference between patients with and without pancreatic fistula concerning to the incidence of DGE (15.8% and 8.7% in patients with and without pancreatic fistula, respectively; $P = 0.3812$). All patients (n = 3) with intra-abdominal hemorrhage in this study were classified as grade B according to the criteria of ISGPS.[32] Although 1 patient in the PpPD group and 2 patients in PrPD group had intra-abdominal bleeding complicated by pancreatic fistula, complete hemostasis was achieved by interventional radiographic techniques. Reoperation rate in this study was 0.8% (1 of the 130 patients), and 1 patient underwent a reoperation requiring drainage on postoperative day (POD) 7 for pancreatic fistula. The postoperative course was uneventful and discharged on POD 40. The mortality rate in this study was 0.8% (1 of the 130 patients). One patient in the PrPD group died because of nonobstructive membrane ischemia.

TABLE 4. Postoperative Complications and Outcomes

	PpPD (n = 64)	PrPD (n = 66)	*P*
Pancreatic fistula*	19 (29.6%)	19 (28.8%)	0.9999
Grade A	11 (17.1%)	11 (16.7%)	
Grade B	7 (10.9%)	5 (7.6%)	
Grade C	1 (1.6%)	3 (4.5%)	
Intra-abdominal abscess	8 (12.5%)	6 (9.1%)	0.7309
Intra-abdominal hemorrhage	1 (1.6%)	2 (3.0%)	0.9999
Intraabdominal hemorrhage	1 (1.6%)	2 (3.0%)	0.9999
Grade A	0 (0%)	0 (0%)	
Grade B	1 (1.6%)	2 (3.0%)	
Grade C	0 (0%)	0 (0%)	
Wound infection	2 (3.1%)	2 (3.0%)	0.9999
Pulmonary complications	1 (1.6%)	2 (3.0%)	0.9999
NOMI	0 (0%)	1 (1.5%)	0.9999
Percutaneous drainage†	8 (12.5%)	6 (9.1%)	0.7309
Reoperation‡	0 (0%)	1 (1.5%)	0.9999
Mortality§	0 (0%)	1 (1.5%)	0.9999

*Pancreatic fistula is defined according to the International Study Group of Pancreatic Surgeons.

†Percutaneous drainage done as postoperative management of intra-abdominal abscess related to pancreatic fistula.

‡One patient underwent reoperation requiring drainage for pancreatic fistula.

§One patient died because of nonobstructive membrane ischemia (NOMI).

TABLE 5. Long-Term Outcomes Between PpPD and PrPD

	PpPD (n = 64)	PrPD (n = 66)	*P*
Quality of life			
Total FACT-Ga score, range 0–184			
1 mo after surgery	119.9 ± 24.3	120.4 ± 29.7	0.9205
3 mo after surgery	132.3 ± 21.3	125.4 ± 26.8	0.1630
6 mo after surgery	139.1 ± 22.9	139.6 ± 21.4	0.9140
FACT-Ga subscale, range 0–76			
1 mo after surgery	48.3 ± 12.3	49.2 ± 16.6	0.7479
3 mo after surgery	55.9 ± 10.2	53.9 ± 13.3	0.3935
6 mo after surgery	59.6 ± 11.0	60.1 ± 11.3	0.8137
Change of body weight, kg			
Before operation	54.9 ± 10	55.0 ± 9	0.9335
1 mo after surgery	50.0 ± 10	0.0 ± 8	0.8547
3 mo after surgery	49.8 ± 10	48.8 ± 8	0.5624
6 mo after surgery	50.9 ± 11	50.0 ± 8	0.4712
Endocrine function			
HbA_{1c},* %			
Before operation	5.8 ± 1.3	6.0 ± 1.7	0.4558
3 mo after surgery	5.6 ± 0.7	5.6 ± 0.8	0.9596
6 mo after surgery	5.7 ± 1.0	5.7 ± 1.2	0.8534
New-onset or worsening diabetes†	3/64 (4.7%)	2/66 (3.0%)	0.6777
New diabetes	2	1	
Worsening diabetes	1	1	

*Normal range of HbA_{1c}: 3.8–5.1 g/dL.

†*New-onset diabetes* is defined as diabetes requiring new medical treatment such as diet treatment, oral drug, or insulin. *Worsening diabetes* is defined as diabetes requiring a modification of the medical treatment for deterioration of previously diagnosed diabetes.

Comparison of QOL, Nutritional Status, and Body Weight Change Between PpPD and PrPD

The overall QOL scores from the FACT-Ga scales are presented in Table 5. The highest possible scores for the physical, social, emotional, and functional subscales in FACT-G are 28, 28, 24, and 28, respectively. The highest possible score for the 19-item FACT-Ga subscale is 76. The highest possible score of total FACT-Ga score by combining total FACT-G score and FACT-Ga subscale is 184. No significant differences were found in the results of any subscale score or the total FACT-Ga scores at 1, 3, and 6 months after surgery between PpPD and PrPD.

Moreover, the patients who underwent PpPD and PrPD did not differ significantly in endocrine function or body weight change before surgery and at 1, 3, and 6 months postoperatively (Table 5).

Among serum nutritional parameters as assessment of nutritional status, rapid turnover proteins, such as albumin, prealbumin, transferrin, and retinol-binding protein, were decreased at 1 month after surgery. The levels were gradually restored thereafter and recovered to baseline or higher than the preoperative levels at 6 months after surgery. The changes in those parameters were similar in the 2 groups (Table 6).

DISCUSSION

The reported overall incidence of DGE according to the new definitions from ISGPS is 33% to 47%.[15,16,32] In previous studies, the pathogenesis of DGE after PpPD has been thought to include several factors, such as (1) antroduodenal ischemia,[20,33] (2) gastric atony caused by vagotomy,[34] (3) pylorospasm,[17–19] (4) absence of gastrointestinal hormone,[35] (5) gastric dysrhythmia secondary to other complications such as pancreatic fistula,[12,14,36–39] and (6) antroduodenal congestion.[21] Operative techniques using antecolic reconstruction for duodenojejunostomy[24] and postoperative management using erythromycin[20,35] were reported to reduce the incidence of DGE. However, the relatively high incidence of DGE after PpPD remains unsolved and we should consider ways to improve the surgical technique to decrease the incidence of DGE.

None of the 139 eligible patients in this study had lymph nodes metastasis of the peripylorus region. However, infrapyloric lymph nodes metastasis in pancreatic head carcinoma was reported to be 12%.[40] Therefore, the sampling or dissection of the peripylorus lymph nodes should be needed in patients with pancreatic head carcinoma. In the present study, we hypothesized that preservation of the pylorus ring is a risk factor for DGE and assessed whether resection of the pylorus ring with preservation of nearly the entire stomach (designated as PrPD) would significantly reduce the incidence of DGE compared with that in conventional PpPD. The results confirmed our hypotheses with the DGE rate of 17.2% in PpPD compared with that of 4.5% in PrPD ($P = 0.0244$). This is the first RCT to clarify that PrPD reduces the incidence of DGE compared with PpPD. If such reduced incidence of DGE is achieved by PrPD, one would expect a shorter hospital stay in the PrPD group. However, postoperative hospital stay in both groups may be longer than that observed in the Western countries. The Japanese health care system is different from the Western countries. Therefore, comparing lengths of postoperative hospital stay is difficult between Japan and the Western countries. Several studies proposed that gastric dysrhythmia secondary to other abdominal complications, such as pancreatic fistula or intra-abdominal abscess, induced the incidence of DGE.[12,14,36–39] In the present study, we found no significant differences between PpPD and PrPD in the incidence of clinically relevant pancreatic fistula or intra-abdominal abscess. Therefore, other postoperative complications had no bias or influence on the incidence of DGE in this study evaluating the 2 procedures. Many pancreatic surgeons believe that DGE after PD is

TABLE 6. Nutritional Status Between PpPD and PrPD

	PpPD (n = 64)	PrPD (n = 66)	P
Albumin,* g/dL			
Before operation	4.1 ± 0.5	4.0 ± 0.5	0.6493
1 mo after surgery	3.6 ± 0.6	3.7 ± 0.5	0.5425
3 mo after surgery	3.9 ± 0.6	3.8 ± 0.6	0.2810
6 mo after surgery	4.0 ± 0.4†	3.9 ± 0.4†	0.4153
Prealbumin,‡ g/dL			
Before operation	22.2 ± 7.1	21.0 ± 6.3	0.3192
1 mo after surgery	15.4 ± 5.4	15.2 ± 4.8	0.7877
3 mo after surgery	19.0 ± 5.9	17.4 ± 4.6	0.1147
6 mo after surgery	21.0 ± 5.0†	19.4 ± 5.7†	0.0944
Transferrin,§ mg/dL			
Before operation	233 ± 49	233 ± 42	0.9892
1 mo after surgery	197 ± 47	197 ± 47	0.9694
3 mo after surgery	225 ± 52	213 ± 59	0.2532
6 mo after surgery	252 ± 52†	232 ± 57†	0.0587
Retinol-binding protein, • mg/dL			
Before operation	3.7 ± 1.4	3.4 ± 1.2	0.2089
1 mo after surgery	2.4 ± 0.9	2.3 ± 0.9	0.5518
3 mo after surgery	2.9 ± 1.0	2.6 ± 1.0	1003
6 mo after surgery	3.1 ± 1.1†	3.0 ± 1.2†	6579

*Normal range of albumin: 3.8–5.1 g/dL.
†The level at 6 months after surgery recovered to the baseline or higher than the preoperative level.
‡Normal range of prealbumin: 22–40 mg/dL.
§Normal range of transferrin: 200–400 mg/dL.
•Normal range of retinol-binding protein: 2.4–7 mg/dL.

caused by local and systemic septic complications. This study again demonstrates that there are complication-unrelated mechanisms for DGE.

As for prophylactic management of pylorospasm due to denervation after PpPD, 2 reports described the operative technique including the mechanical dilatation of the pylorus ring and pyloromyotomy.[18,19] It has been proposed that the addition of pyloric dilatation in PpPD reduces the incidence of DGE from 26% to 6.5% ($P < 0.05$) compared with conventional that in PpPD.[18] On the other hand, the addition of pyloromyotomy in PpPD reduces the incidence of DGE from 21% to 2% ($P < 0.01$) compared with that in conventional PpPD.[19] However, these 2 studies were not RCTs. To avoid bias issues, RCTs should be performed to determine the better surgical procedure.

The ^{13}C-acetate breath test is a simple and excellent indirect test for gastric emptying.[26] In particular, the time of peak $^{13}CO_2$ content has been reported to be a more useful marker reflecting gastric emptying.[28] To our knowledge, no reports have evaluated gastric emptying by the ^{13}C-acetate breath test in patients with pancreatic head resection. In this study, gastric emptying assessed by the ^{13}C-acetate breath test at 1, 3, and 6 months after surgery was significantly delayed in patients undergoing PpPD compared with that in those undergoing PrPD. This result of the ^{13}C-acetate breath test supported the hypothesis that the incidence of DGE was significantly lower in PrPD (4.5%) than in PpPD (17.1%). On the other hand, rapid gastric emptying in the ^{13}C-acetate breath test seems to reflect dumping syndrome after gastrectomy. However, only 1 of 66 patients (1.5%) in the PrPD group had dumping syndrome, and no patient undergoing PpPD had this complication.

Pylorus-preserving pancreatoduodenectomy has been reported to reduce syndromes occurring after gastrectomy, including dumping syndrome, diarrhea, and poor recovery of body weight and to afford patients a better nutritional status compared with that in PD with antrectomy.[8–12] Pylorus-resecting pancreatoduodenectomy may lead to gastrectomy syndromes because of resecting the pylorus ring, as done in PD with antrectomy. Moreover, no reports have evaluated QOL for syndromes after gastrectomy or gastric emptying function between patients with preservation and resection of the pylorus ring in PD. The gastric cancer–specific FACT-Ga questionnaire, which consists of the 27 items from the FACT-G and 19 gastric cancer–specific items, was reported to reflect postgastrectomy syndromes.[29] The incidence of DGE greatly influences postgastrectomy syndrome or postoperative gastric emptying function. We believe that FACT-Ga is the best QOL questionnaire to evaluate the differences of QOL in patients with or without DGE. Therefore, FACT-Ga questionnaire was chosen in this RCT to compare PpPD and PrPD regarding postgastrectomy syndromes or gastric emptying function. In this study, no significant differences occurred in postgastrectomy syndromes or sensation of gastric fullness between PpPD and PrPD. More than 95% of the stomach is preserved in PrPD, and the stomach pooling ability is preserved in PrPD in the same way as in PpPD, although the pylorus ring was resected. However, the next step is to clarify whether PrPD is a better surgical procedure compared with conventional PD with antrectomy.

In conclusion, this study suggested that PrPD can lead to a significant reduction in the incidence of DGE compared with conventional PpPD. The patients enrolled in this study will be followed carefully in terms of nutritional status and QOL for 1 year and 2 years postoperatively and evaluated for the better procedure.

REFERENCES

1. Traverso LW, Longmire WJ. Preservation of the pylorus in pancreaticoduodenectomy. *Surg Gynecol Obstet.* 1978;146:959–962.
2. Lin PW, Lin YJ. Prospective randomized comparison between pylorus preserving and standard pancreaticoduodenectomy. *Br J Surg.* 1999;86:603–607.
3. Seiler CA, Wagner M, Sadowski C, et al. Randomized prospective trial of pylorus-preserving vs classic duodenopancreatectomy (Whipple procedure): initial clinical results. *J Gastrointest Surg.* 2000;4:443–452.
4. Tran KTC, Smeenk HG, van Eijck CHJ, et al. Pylorus preserving pancreaticoduodenectomy versus standard Whipple procedure. A prospective, randomized, multicenter analysis of 170 patients with pancreatic and periampullary tumors. *Ann Surg.* 2004;240:738–745.
5. Seiler CA, Wagner M, Bachmann CA, et al. Randomized clinical trial of pylorus-preserving duodenopancreatectomy versus classical Whipple resection—long term results. *Br J Surg.* 2005;92:547–556.
6. Lin PW, Shan YS, Lin YJ, et al. Pancreaticoduodenectomy for pancreatic head cancer: PPPD versus Whipple procedure. *Hepatogastroenterology.* 2005;52:1601–1604.
7. Diener MK, Knaebel HP, Heukaufer C, et al. A systematic review and meta-analysis of pylorus-preserving versus classical pancreaticoduodenectomy for surgical treatment of periampullary and pancreatic carcinoma. *Ann Surg.* 2007;245:187–200.
8. Traverso LW, Longmire WJ. Preservation of the pylorus in pancreaticoduodenectomy: a follow-up evaluation. *Ann Surg.* 1980;192:306–310.
9. Jimenez RE, Femandez-del Castillo C, Rattner DW, et al. Outcome of pancreaticoduodenectomy with pylorus preservation or with antrectomy in the treatment of chronic pancreatitis. *Ann Surg.* 2000;231:293–300.
10. Brasssch JW, Deziel DJ, Rossi RL, et al. Pyloric and gastric preserving pancreatic resection. Experience with 87 patients. *Ann Surg.* 1986;204:411–418.
11. Hunt DR, McLean R. Pylorus-preserving pancreatectomy: functional results. *Br J Surg.* 1989;76:173–176.
12. van Berge Henegouwewn MI, van Gulik TM, De Wit LT, et al. Delayed gastric emptying after standard pancreaticoduodenectomy versus pylorus-preserving pancreaticoduodenectomy: an analysis of 200 consecutive patients. *J Am Coll Surg.* 1997;185:373–379.

13. Yeo CJ, Cameron JL, Sohn TA, et al. Six hundred fifty consecutive pancreaticoduodenectomy in the 1990s: pathology, complications, and outcomes. *Ann Surg*. 1997;226:248–257.
14. Horstmann O, Markus PM, Ghadimi MB, et al. Pylorus preservation has no impact on delayed gastric emptying after pancreatic head resection. *Pancreas*. 2004;28:69–74.
15. Akizuki E, Kimura Y, Nobuoka T, et al. Reconsideration of postoperative oral intake tolerance after pancreaticoduodenectomy—prospective consecutive analysis of delayed gastric emptying according to the ISGPS definition and the amount of dietary intake. *Ann Surg*. 2009;249:986–994.
16. Hashimoto Y, Traverso LW. Incidence of pancreatic anastomotic failure and delayed gastric emptying after pancreatoduodenectomy in 507 consecutive patients: use of a web-based calculator to improve homogeneity of definition [published online ahead of print December 15, 2009]. *Surgery*. 2010;147: 503–515.
17. Gauvin JM, Sarmiento JM, Sarr MG. pylorus-preserving pancreaticoduodenectomy with complete preservation of the pyloroduodenal blood supply and innervation. *Arch Surg*. 2003;138:1261–1263.
18. Fischer CP, Hong JC. Method of pyloric reconstruction and impact upon delayed gastric emptying and hospital stay after pylorus-preserving pancreaticoduodenectomy. *J Gastrointest Surg*. 2006;10:215–219.
19. Kim DK, Hindenburg AA, Sharma SK, et al. Is pylorospasm a cause of delayed gastric emptying after pylorus-preserving pancreaticoduodenectomy? *Ann Surg Oncol* 2005;12:222–227.
20. Ohwada S, Satoh Y, Kawate S, et al. Low-dose erythromycin reduces delayed gastric emptying and improves gastric motility after Billroth I pylorus-preserving pancreaticoduodenectomy. *Ann Surg*. 2001;234:668–674.
21. Kurosaki I, Hatakeyama K. Preservation of the left gastric vein in delayed gastric emptying after pylorus-preserving pancreaticoduodenectomy. *J Gastrointest Surg*. 2005;9:846–852.
22. Tani M, Kawai M, Terasawa H, et al. Complication with reconstruction procedure in pylorus-preserving pancreaticojejunostomy. *World J Surg*. 2005;29:881–884.
23. Tani M, Onishi H, Kinosita H, et al. The evaluation of duct-to mucosal pancreaticojejunostomy in pancreaticoduodenostomy. *World J Surg*. 2005;29:76–79.
24. Tani M, Terasawa H, Kawai M, et al. Improvement of delayed gastric emptying in pylorus-preserving pancreaticoduodenectomy: results of a prospective, randomized, controlled trial. *Ann Surg* 2006;243:316–320.
25. Kawai M, Tani M, Terasawa H, et al. Early removal of prophylactic drains reduces the risk of intra-abdominal infections in patients with pancreatic head resection: prospective study for consecutive 104 patients. *Ann Surg*. 2006;244:1–7.
26. Braden B, Adams S, Duan LP, et al. The [13C]acetate breath test accurately reflects gastric emptying of liquids in both liquid and semisolid test meals. *Gastroenterology*. 1995;108:1048–1055.
27. Nakata K, Aoyama N, Nakagawa M, et al. The present and the future in gastric emptying study assessed by ^{13}C-acetate breath test—with special reference to the standardization of the method [in Japanese]. *J Smooth Muscle Res*. 2002;6:J75–J91.
28. Urita Y, Hike K, Torii N, et al. Efficacy of lactulose plus ^{13}C-acetate breath test in the diagnosis of gastrointestinal motility disorders. *J Gastroenterol*. 2002;37:442–448.
29. Eremenco SL, Cashy J, Webster K, et al. FACT-Gastric: a new international measure of QOL in gastric cancer. *ASCO Proc*. 2004;23:755. Abstract 8123.
30. Wente MN, Bassi C, Dervenis C, et al. Delayed gastric emptying (DGE) after pancreatic surgery: a suggested definition by the International Study Group of Pancreatic Surgery (ISGPS). *Surgery*. 2007;142:761–768.
31. Bassi C, Dervenis C, Butturini G, et al. Postoperative pancreatic fistula: an international study group (ISGPF) definition. *Surgery*. 2005;138:8–13.
32. Wente MN, Veit JA, Bassi C, et al. Postpancreatectomy hemorrhage (PPH)—an International Study Group of Pancreatic Surgery (ISGPS) definition. *Surgery*. 2007:142,20–25.
33. Park JS, Hwang HK, Kim JK, et al. Clinical validation and risk factors for delayed gastric emptying based on the International Study Group of Pancreatic Surgery (ISGPS) Classification. *Surgery*. 2009;146:882–887.
34. Itani KM, Coleman RE, Meyers WC, et al. Pylorus-preserving pancreaticoduodenectomy. A clinical and physiologic appraisal. *Ann Surg*. 1986;204: 655–664.
35. Kobayasi I, Miyachi M, Kanai M, et al. Different gastric emptying of solid and liquid meals after pylorus-preserving pancreaticoduodenectomy. *Br J Surg*. 1998;85:927–930.
36. Yeo CJ, Barry MK, Sauter PK, et al. Erythromycin accelerates gastric emptying following pancreaticoduodenectomy: a prospective, randomized placebo-controlled trial. *Ann Surg*. 1993;218:229–238.
37. Raty S, Sand J, Lantto E, et al. Postoperative acute pancreatitis as a major determinant of postoperative delayed gastric emptying after pancreaticoduodenectomy. *J Gastrointest Surg*. 2006;10:1131–1139.
38. Riediger H, Makowiec F, Schareck WD, et al. Delayed gastric emptying after pylorus-preserving pancreaticoduodenectomy is strongly related to other postoperative complications. *J Gastrointest Surg*. 2003;7:758–765.
39. Miedema BW, Sarr MG, van Heerden JA, et al. Complications following pancreaticoduodenectomy: current management. Arch Surg. 1992;127:945–949.
40. Sakai M, Nakao A, Kaneko T, et al. Para-aortic lymph node metastasis in carcinoma of the head of the pancreas. *Surgery*. 2005; 137:606–611.

uicc
global cancer control

IJC
International Journal of Cancer

Re-expression of CEACAM1 long cytoplasmic domain isoform is associated with invasion and migration of colorectal cancer

Junji Ieda[1], Shozo Yokoyama[1], Koichi Tamura[1], Katsunari Takifuji[1], Tsukasa Hotta[1], Kenji Matsuda[1], Yoshimasa Oku[1], Toru Nasu[1], Shigehisa Kiriyama[1], Naoyuki Yamamoto[1], Yasushi Nakamura[2], John E. Shively[3] and Hiroki Yamaue[1]

[1] Second Department of Surgery, Wakayama Medical University School of Medicine, Wakayama, Japan
[2] Department of Clinical Laboratory Medicine, Wakayama Medical University School of Medicine, Wakayama, Japan
[3] Department of Immunology, Beckman Research Institute of the City of Hope, Duarte, CA

Carcinoembryonic antigen-related cell adhesion molecule 1 (CEACAM1) is known to be downregulated at the transcriptional level in adenoma and carcinoma. Recent reports have shown that CEACAM1 is overexpressed at protein level in colorectal cancer and correlated with clinical stage. The reason why colorectal cancer cells re-expressed CEACAM1 remains unclear. The aim of our study was to clarify the implication of CEACAM1 re-expression in colorectal cancer. Immunohistochemical analyses were conducted with CEACAM1 long (CEACAM1-L) or short (CEACAM1-S) cytoplasmic domain-specific antibodies on clinical samples from 164 patients with colorectal cancer. The risk factors for metastasis and survival were calculated for clinical implication of CEACAM1 re-expression. Invasion chamber and wound healing assays were performed for the effect of CEACAM1 expression on invasion and migration of colorectal cancer cells. CEACAM1-L and CEACAM1-S stained with greater intensity at the invasion front than at the luminal surface of tumors. Differences between the long and short cytoplasmic isoform expression levels were observed at the invasion front. Multivariate analysis showed that CEACAM1-L dominance was an independent risk factor for lymph node metastasis, hematogenous metastasis and short survival. The Kaplan–Meier evaluation demonstrated that CEACAM1-L dominance was associated with shorter survival time ($p < 0.0001$). In the invasion chamber and wound healing assays, CEACAM1-L promoted invasion and migration. Re-expression of CEACAM1 is observed at the invasion front of colorectal cancer. CEACAM1-L dominance is associated with metastasis and shorter survival of the patients with colorectal cancer. CEACAM1-L dominance is important for colorectal cancer cells invasion and migration.

Carcinoembryonic antigen-related cell adhesion molecule 1 (CEACAM1) is a cell adhesion molecule, formerly known as CD66a or biliary glycoprotein 1, which belongs to the carcinoembryonic antigen family and a subgroup of the immunoglobulin (Ig) superfamily.[1] CEACAM1 is known to be a tumor suppressor, which acts as a regulator of apoptosis.[2] The expression of CEACAM1 is downregulated in malignant tissues derived from colon,[3] breast,[4] prostate[5] and endometrium.[6] On the other hand, upregulation of CEACAM1 is associated with a short survival and metastatic spread in patients with cutaneous malignant melanoma[7] and in lung adenocarcinoma.[8]

In colorectal cancers, the mRNA level of CEACAM1 was downregulated in colorectal adenomas and adenocarcinomas.[3] However, recent reports have demonstrated that the protein expression of CEACAM1 is upregulated in adenocarcinomas,[9,10] and that the intensity of the entire CEACAM1 protein was correlated with the stage of TNM classification,[10] but not significantly correlated with the overall survival or disease-free survival.[9] No study has so far determined the reason for the re-expression of CEACAM1 in colorectal cancer.

CEACAM1 has alternatively spliced isoforms with either three or four Ig-like extracellular domains and a long (CEACAM1-L) or a short (CEACM1-S) cytoplasmic tail.[11] The long cytoplasmic domain contains two immunoreceptor tyrosine-based inhibitory motifs (ITIMs) that can be phosphorylated by Src kinases[12] and, once phosphorylated, can bind the SHP-1 and-2 phosphatase.[13] The long cytoplasmic domain also binds actin and tropomyosin.[14] In contrast, the short cytoplasmic domain isoform, with 12–14 amino acids and no ITIMs, can bind actin, tropomyosin, annexin II and calmodulin.[14] Therefore, the long and short cytoplasmic domain isoforms play distinct roles in the regulation of cytoskeleton assembly and signaling pathways. The determination of the CEACAM1 cytoplasmic domain isoform expression levels

Key words: CEACAM1, colorectal cancer, invasion, cytoplasmic domain, isoform balance
Abbreviations: Mod: moderately differentiated adenocarcinoma; CEACAM1-L dominance: CEACAM1-long isoform dominance; HR: hazard ratio; CI: confidential linterval.
All authors have no disclosures of competing interests
Grant sponsor: Ministry of Education, Culture, Sports, Science, and Technology, Japan; Grant number: 20591554; Grant sponsor: Takeda Science Foundation, Japan
DOI: 10.1002/ijc.26072
History: Received 28 Oct 2010; Accepted 15 Feb 2011; Online 16 Mar 2011
Correspondence to: Shozo Yokoyama, 811-1 Kimiidera, Wakayama 641-8510, Japan, Tel.: +81-73-441-0613, Fax: +81-73-446-6566, E-mail: yokoyama@wakayama-med.ac.jp

can provide new information regarding the implication of re-expression of colorectal cancer.

In our study, we presented, by using CEACAM1 long or short specific antibodies, re-expression of CEACAM1 distributed at the invasion front, suggesting that CEACAM1 re-expression was involved in cancer cells invasion and migration. Also, we showed that the relative expression levels of the CEACAM1 cytoplasmic isoforms were correlated with invasion and migration of colorectal cancer cells.

Material and Methods

Patients

One hundred and sixty-four patients with colorectal cancer who underwent surgery were enrolled in this study between January 2002 and December 2003 in Wakayama Medical University Hospital (WMUH). The patients included 26 Stage I, 63 Stage II, 47 Stage III and 28 Stage IV colorectal carcinomas based on the TNM classification. The mean age of the patients was 65.3 ± 11.8 years, and there were 95 male and 69 female subjects. The tumors were resected from either the colon (n = 90) or the rectum (n = 74). The follow-up period was 5 years. Stage III and IV patients received 5-fluorouracil-based postoperative chemotherapy, whereas Stage I and II patients received no chemotherapy. Our study was approved by the Human Ethics Review Committee of WMUH.

Generation of polyclonal antibodies specific for CEACAM1-L and CEACAM1-S

To generate antibodies to the short cytoplasmic domain of CEACAM1, the peptide whose sequence was the entire short form 12 amino acid sequence with two lysines at the N terminus (KKHFGKTGSSGPLQ) was conjugated to keyhole limpet hemocyanin with glutaraldehyde and immunized into a mouse.

To generate antibodies to the long form, the C-terminal peptide with two lysines at the N-terminal end (KK PSLTATEIIY SEVKKQ) was conjugated to keyhole limpet hemocyanin with glutaraldehyde and immunized into a rabbit.

Immunohistochemistry

Immunohistological staining using the streptavidin-biotin methods was performed. Tissue sections (4-μm thick) were prepared from formalin-fixed paraffin-embedded blocks. Sections were deparaffinized and autoclaved at 121°C for 10 min in 0.1 M citrate buffer (pH 6.0). Endogenous peroxidase activities were blocked by incubation in 3% hydrogen peroxide for 5 min at room temperature. The slides were washed with PBS buffer solution and incubated with serum-free protein blocking solution (X0909, DAKO, USA) for 10 min at room temperature. Thereafter, the sections were incubated with the primary antibodies, rabbit anti-human CEACAM-long-specific polyclonal antibodies (1:1,000) or mouse anti-human CEACAM-short (1:500)-specific polyclonal antibodies for 18 hr at 4°C. The specificity and selectivity of CEACAM-long-specific antibodies or CEACAM-short-specific antibodies were confirmed by Western blotting analyses and immunohistochemistry in Figure 1. A biotinylated secondary antibody and peroxidase-conjugated streptavidin from Nichirei Histofine MAX-PO(M) kit (Nichirei, Japan) were applied for 30 min at room temperature. Finally, the sections were incubated in 3,3′-diaminobenzidine for 10 min, followed by hematoxylin counterstaining and slide mounting. All specimens were blindly reviewed twice by three individuals including a pathologist (J.I., S.Y. and Y.N.). If discrepancies arose, the specimens were discussed to achieve a consensus while being viewed with a multihead microscope. The correlation between the CEACAM1 isoform balance and the clinicopathological characteristics of these patients was evaluated. All pictures excluding fluorescence immunohistochemistry were acquired using a Nikon Eclipse 80i (Nikon, Japan), with the NIS-Elements D 2.30 software program (Nikon, Japan).

To investigate the specificity of the polyclonal antibodies, we performed the proximity ligation assay (Duolink™ *in situ* PLA, Olink Bioscience, Uppsala, Sweden) for paraffin-embedded tissue slides according to the manufacture's instructions. We use a rabbit anti-CEACAM1-L polyclonal antibody and a mouse anti-CEACAM1 monoclonal antibody (29H2) as primary antibodies. Subsequently, slides were visualized using a Biorevo BZ-9000 fluorescence microscope (Keyence, Osaka, Japan).

Cells lines

Two human colorectal cancer cell lines were used in our study. LS174T and HT29 cells were purchased from the American Type Culture Collection (Manassas, VA). LS174T cells were maintained in Eagle's minimum essential medium (WAKO, Tokyo, Japan) supplemented with 10% fetal bovine serum (FBS) (GIBCO, Grand Island, NY), 100 U/ml of penicillin G, 100 μg/ml of streptomycin and 0.25 μg/ml of amphotericin B (GIBCO) at 37°C in a humidified 5% CO_2 atmosphere. HT29 cells were maintained in McCoy's 5A (GIBCO) medium containing 10% FBS (GIBCO), 100 U/ml of penicillin G, 100 μg/ml of streptomycin and 0.25 μg/ml of amphotericin B (GIBCO) at 37°C in a humidified 5% CO_2 atmosphere.

Transfection and RNA interference

CEACAM1-4L or -4S cDNA cloned into the pH-β actin vector[15] (0.8 μg) was mixed with 1 μl of Lipofectamine 2000 (Invitrogen) in a final volume of 100 μl of Opti-MEM medium and was added to LS174T and HT29 cells grown to 40% confluence in 24-well plates. Forty-eight hours after transfection, G418 solution (Roche, Basel, Switzerland) was added in the appropriate concentration. The stably transfected cells were maintained in each medium as described. Short hairpin RNA (shRNA) plasmids designed to target CEACAM1 were synthesized by SABiosciences (Frederick, MD) as follows: insert sequence CCA CAA ATG ACA CTG

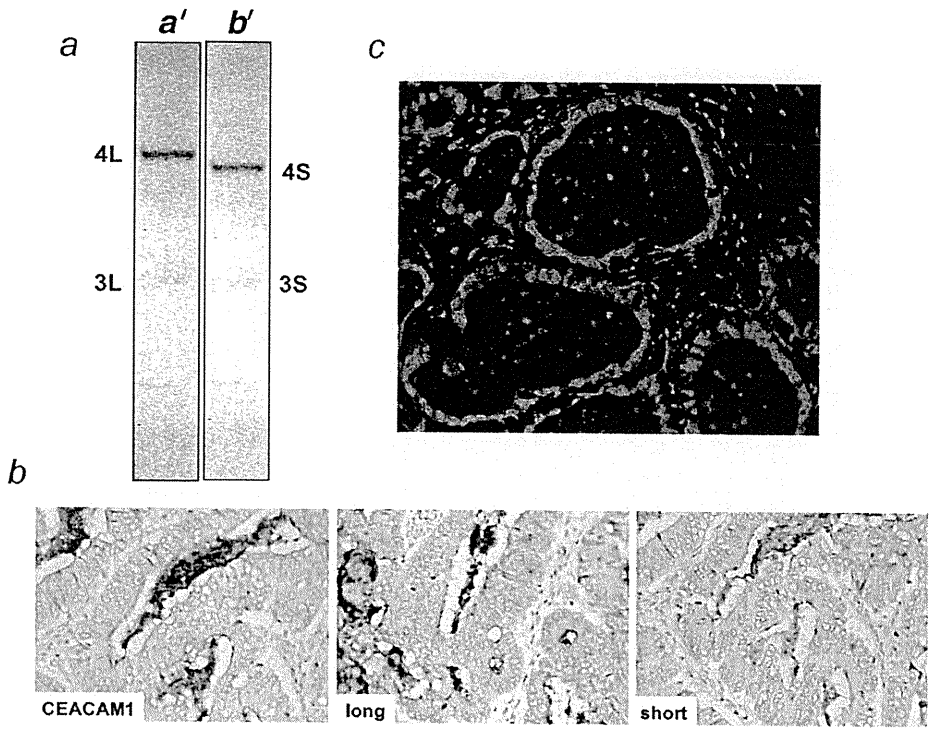

Figure 1. Specificity of polyclonal anti-CEACAM1-L and -S antibodies. (*a*) Western blot with a clinical sample of colon cancer showed that the antibodies have no cross reactivity with other proteins. (*a'*) Western blot with CEACAM1-L-specific polyclonal antibodies; (*b'*) Western blots with CEACAM1-S-specific polyclonal antibodies. 4L: CEACAM1-4L; 4S: CEACAM1-4S; 3L: CEACAM1-3L; 3S: CEACAM1-3S. (*b*) All three antibodies, mouse anti-CEACAM1 monoclonal antibodies (29H2, CEACAM1), rabbit anti-CEACAM1-L polyclonal antibodies (Long) and mouse anti-CEACAM1-S antibodies (Short), had same staining pattern at the luminal surface of the tumor. (*c*) Proximity ligation assay with DAPI staining (blue) showed colocalization (red) of mouse monoclonal anti-CEACAM1 antibodies and rabbit polyclonal anti-CEACAM1-L antibodies at the luminal surface of the tumor.

GAA TCT and gga atc tca ttc gat gca tac (Negative control). Each plasmid (0.8 μg) was transfected as described above.

Reverse transcriptase-polymerase chain reaction

Total RNA was prepared using the RNeasy mini kit (Qiagen, Hilden, Germany) and was subjected to reverse transcription using the Reverse Transcription System (Promega, Madison, WI). Reverse transcriptase-polymerase chain reaction was performed using the *TaKaRa Taq* enzyme (Takara, Shiga, Japan). The PCR conditions were 35 cycles of denaturation, annealing and extension (94°C for 30 sec, 55°C for 30 sec and 72°C for 1 min). The primers for the human CEACAM1 gene were as follows: sense primer: 5′-CTG CAA CAG GAC CAC AGT CAA G-3′ and antisense primer: 5′-GCT GGG CTT CAA AGT TCA GGG T-3′, which encompass the extracellular B1 domain to the cytoplasmic domain and could amplify four alternatively spliced mRNA transcripts of CEACAM1 (CEACAM1-3L, -3S, -4L and -4S).[16,17] The PCR products were visualized by electrophoresis on an agarose gel stained with ethidium bromide.

Western blot analysis

After quantifying the protein, the samples were prepared for sodium dodecyl sulfate-polyacrylamide gel electrophoresis. In each lane, 25 μl of each sample was loaded and separated in a precast polyacrylamide gel (Invitrogen, Carlsbad, CA). Subsequently, proteins were electrotransferred to a nitrocellulose membrane (BIO-RAD, Hercules, CA). After blocking the membrane with 5% electrophoresis-grade nonfat milk, primary and secondary antibodies were incubated for 30 min each in a 5% milk solution. Immune complexes were visualized by incubating the membranes with an HRP-conjugated anti-mouse or anti-rabbit antibody using the ECL detection reagent (GE healthcare, Little Chalfont, Buckinghamshire, UK). The primary antibodies (mouse monoclonal T84.1, diluted 1:1,000; rabbit polyclonal CEACAM1-L, diluted 1:1,000 and mouse polyclonal CEACAM1-S, diluted 1:1,000) were produced by J.E.S., Beckman Research Institute of the City of Hope, CA. The secondary antibodies were sheep anti-mouse IgG conjugated to HRP and donkey anti-rabbit IgG conjugated to HRP (diluted 1:1,000, GE Healthcare).

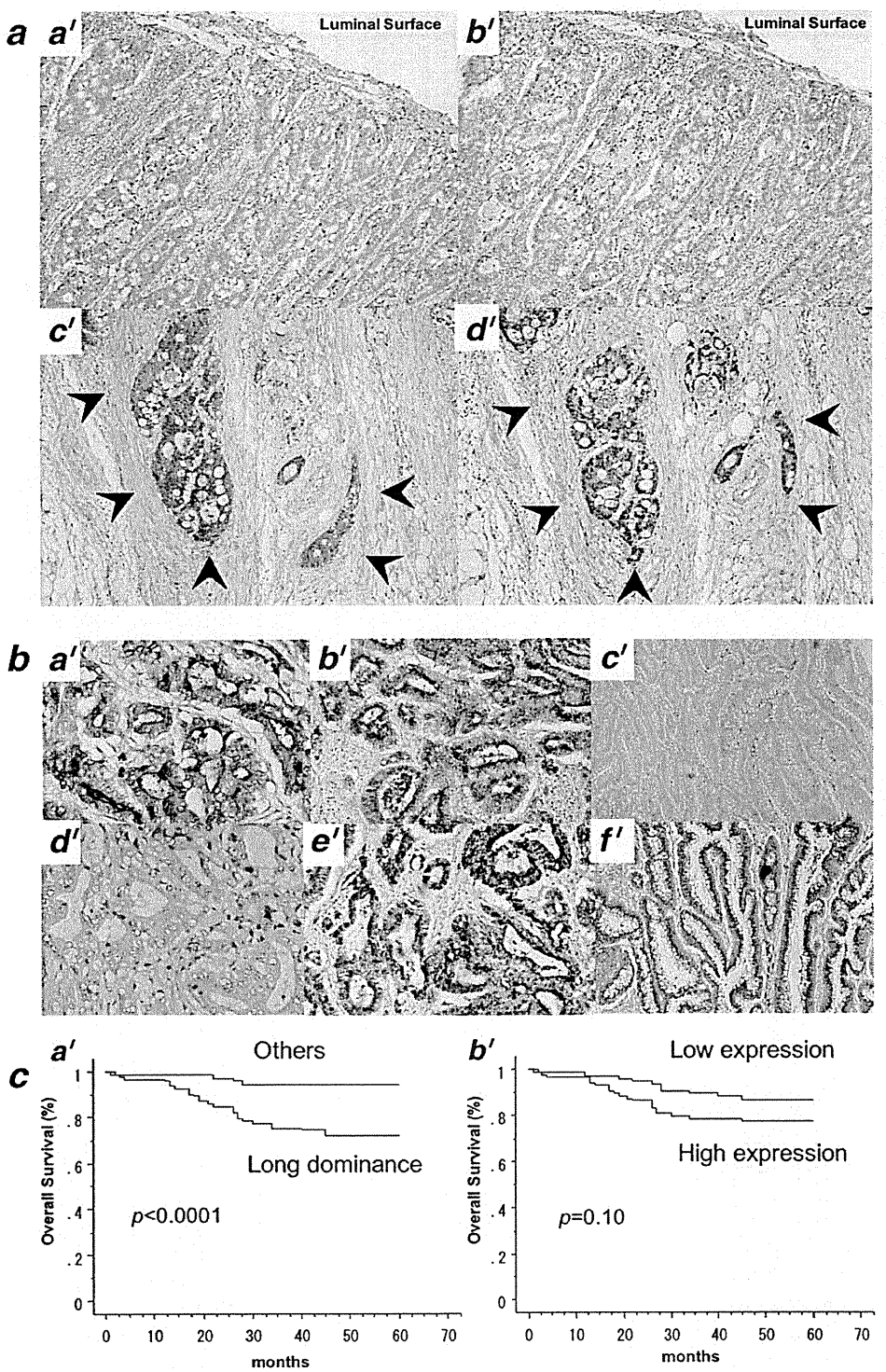
a
a′
Luminal Surface
b′
Luminal Surface
c′
d′
b
a′
b′
c′
d′
e′
f′
c
a′
Others
Long dominance
p<0.0001
Overall Survival (%)
months
b′
Low expression
High expression
p=0.10
Overall Survival (%)
months

Figure 2.

In vitro invasion assay

The number of invading cells was assayed in the membrane invasion culture system using an 8-μm pore size PET membrane coated with Matrigel (24-well, BD Biosciences). Cells were seeded at 1×10^4 cells per 500 μl of growth medium on the Matrigel layer. The bottom of the well was filled with the culture medium, and the plates were incubated at 37°C in a humidified 5% CO_2 atmosphere for 22 hr. After incubation, the Matrigel layer was removed with a cotton swab to remove the Matrigel and the noninvading cells. The cells on the lower surface of the membrane were stained with Diff Quick (Sysmex, Kobe, Japan). The invading cells were counted with a microscope. Each measurement was performed in quadruplicate.

Wound healing assay

The cells were each added to six-well plates, allowed to form confluent monolayers and were serum starved overnight. An artificial wound was created onto the cells monolayer with a sterile plastic 200-μl micropipette tip to generate one homogeneous wound in each well. After wounding, the culture medium was removed, and cells were washed at least twice to eliminate detached cells. Wound closure was photographed immediately, 48 hr after wounding at the same spot using an inverted microscope equipped with a digital camera. Each measurement was performed in quadruplicate.

Statistical analysis

Each clinicopathological factor was separately assessed using the chi-square test. The factors determined to be significant by the chi-square test were analyzed by a multivariate logistic regression, and an odds ratio with a 95% confidence interval was calculated for each factor. The Kaplan–Meier method was used to estimate the survival from colorectal cancer, and the log-rank test was used to determine the statistical significance. A Cox proportional hazards model was used to assess the risk ratio under simultaneous contributions from several covariates. The associations between discrete variables were assessed using the chi-square test. All data were expressed as the mean ± SD. A p-value of less than 0.05 was considered to be statistically significant. Statistical calculations were performed using the StatView ver.5.0 software program (SAS Institute, Cary, NC).

Results

Specificity and sensitivity of CEACAM1-L and -S polyclonal antibodies

To prove the specificity, we performed the Western blot, immunohistochemistry and proximity ligation assay. Western blot of a clinical sample of colon cancer showed that the antibodies have no cross reactivity with other proteins (Fig. 1*a*). All three antibodies, mouse anti-CEACAM1 monoclonal antibody (29H2), rabbit anti-CEACAM1-L polyclonal antibody and mouse anti-CEACAM1-S antibody, were stained at luminal surface of the tumor (Fig. 1*b*). Proximity ligation assay showed that monoclonal and polyclonal anti-CEACAM1 antibodies were colocalized at the luminal surface of the tumor (Fig. 1*c*).

Expression and distribution of CEACAM1 cytoplasmic domain isoforms

To clarify the distribution of CEACAM1 re-expression, immunohistochemical analyses with CEACAM1-L or CEACAM1-S specific antibodies were performed. Both CEACAM1-L and CEACAM1-S stained with a higher intensity at the invasion front than at the luminal surface of tumors in 149 of 164 patients (91%, Fig. 2*a*), indicating that CEACAM1 re-expression was involved in invasion. There were differences among the patient tumors in the long or short cytoplasmic domain dominance at the invasion front. As there are some heterogeneous CEACAM1 isoform expression patterns, the CEACAM1 expression levels were evaluated with several sections at the invasion front where it was stained most intensely and classified, using the semiquantitative scale, which was modified as described in published study,[4] as: Grade 0, absence; Grade 1, sparse; Grade 2, moderate and Grade 3, strong. The sections were divided into two groups: the CEACAM1-L dominant group, in which CEACAM1-L expression was dominant (Fig. 2*b*, panels *a′* and *d′*), and the second group, in which the expression of the two different domains was equally intense (Fig. 2*b*, panels *b′* and *e′*) or CEACAM1-S expression was dominant (Fig. 2*b*, panels *c′*

Figure 2. Expression pattern of CEACAM1 cytoplasmic isoforms. (*a*) Immunohistochemical analyses revealed that the expression of both CEACAM1-L and -S was more intense at the invasive front than the luminal surface of colorectal cancer tissue. (*a′*) The luminal surface of the tumor was stained with anti-CEACAM1-L antibodies. (*b′*) The luminal surface of the tumor was stained with anti-CEACAM1-S antibodies. (*c′*) The invasion front of the tumor was stained with anti-CEACAM1-L antibodies. (*d′*) The invasion front of the tumor was stained with anti-CEACAM1-S antibodies. Arrowheads indicated the tumor invasion front in *c′* and *d′*. Magnification, ×100. (*b*) Classification of the tumor according to the isoform balance. (*a′*, *b′* and *c′*) The immunostaining using anti-CEACAM1-L antibodies. (*d′*, *e′* and *f′*) The figures using anti-CEACAM1-S antibodies. (*a′*) and (*d′*) were considered to be CEACAM1-L dominant. The other group included the samples in (*b′*) and (*e′*), which showed the same intensity, and (*c′*) and (*f′*), in which CEACAM1-S was dominant. Magnification, ×200. (*c*) Kaplan–Meier estimates of survival. (*a′*) CEACAM1-L dominant group showed a shorter survival than the other group ($p < 0.0001$). (*b′*) There was no significant difference in the overall survival between the high expression group and the low expression group ($p = 0.10$).

Table 1. Univariate analyses of lymph node metastasis and hematogenous metastasis

	Lymph nodes metastasis			Hematogenous metastasis		
	Present	Absent	*p*-value	Present	Absent	*p*-value
Age			0.19			0.72
>66	32	55		14	73	
≤66	36	41		14	63	
Gender			0.083			0.24
Male	34	61		19	76	
Female	34	35		9	60	
Tumor site			0.83			0.53
Colon	38	52		20	70	
Rectum	30	44		8	66	
Differentiation			*0.007*			*0.0067*
Mod	23	15		12	26	
Well	45	81		16	110	
Depth			*0.0015*			*0.0026*
T3,4	63	70		28	105	
T1,2	5	26		0	31	
Lymphatic permeation			*<0.001*			*0.0004*
Present	63	63		28	98	
Absent	5	33		0	38	
Venous permeation			*0.016*			*0.0005*
Present	55	61		27	89	
Absent	13	35		1	47	
CEACAM1 isoform			*<0.0001*			*0.0007*
L dominance	53	41		24	70	
Others	15	55		4	66	

The italic fonts given for *p*-values of less than 0.05.
Abbreviations: Mod: moderately differentiated adenocarcinoma; Well: well-differentiated adenocarcinoma; L dominance: CEACAM1-long isoform dominance.

and *f*). It is noteworthy that 15 patients' tumors with early carcinomas restricted to the mucosa and submucosa weakly expressed both CEACAM1-L and -S, and IHC scores of the tumors were 0 or 1. The patients were divided into two groups: CEACAM1-L dominance ($n = 94$) and CEACAM1-L/S equal expression ($n = 68$) plus CEACAM1-S dominance ($n = 2$). The patients were also divided into two groups based on the expression intensity levels: CEACAM1 high expression ($n = 87$) and low expression ($n = 77$), according to the average score (2.1) of the total score of CEACAM1-L and -S, to address the correlation between CEACAM1-L and -S expression intensity level and malignant potential of colorectal cancer.

CEACAM1 long cytoplasmic domain isoform dominance and metastases

To investigate that CEACAM1 cytoplasmic isoform balance at the invasion front is correlated with lymph node involvement and hematogenous metastases, statistical analyses were performed between CEACAM1 cytoplasmic isoform balance and clinicopathological characteristics. A chi-square test or Fisher's exact test for lymph node metastasis revealed that CEACAM1-L dominance, moderate differentiation, depth of tumor invasion, lymphatic permeation and venous permeation were statistically correlated (Table 1). A multivariate logistic regression analysis for lymph node metastasis revealed CEACAM1-L dominance, depth of tumor and lymphatic permeation to be independent risk factors (Table 2). A chi-square test for hematogenous metastasis revealed that CEACAM1-L dominance, moderate differentiation, depth of tumor, lymphatic permeation and venous permeation were statistically correlated (Table 1). The only independent risk factor in a multivariate logistic regression analysis for hematogenous metastasis was CEACAM1-L isoform dominance (Table 2). These results suggested that re-expression of CEACAM1 long cytoplasmic isoform at the invasion front of colorectal cancer is associated with invasion and metastases of colorectal cancer.

Table 2. Multivariate analyses of lymph node metastasis and hematogenous metastasis

		Lymph node metastasis			Hematogenous metastasis		
Variable	No. of patients	OR	95% CI	*p*-value	OR	95% CI	*p*-value
Depth (T3,T4)	133	3.707	1.184–11.60	0.024			
Lymphatic permeation	126	3.677	1.135–11.911	0.03			
CEACAM1-L dominance	94	4.736	2.215–10.124	<0.0001	4.69	1.465–15.015	0.0092

Abbreviations: CEACAM1-L dominance: CEACAM1-long isoform dominance; OR: odds ratio; CI: confidential interval.

Table 3. Univariate and multivariate analyses of survival

	Univariate analysis			Multivariable analysis		
Variable	HR	95% CI	*p*-value	HR	95% CI	*p*-value
Age (<66)	1.14	0.43–1.80	0.61			
Gender (male)	1.3	0.37–1.61	0.49			
Tumor site (left)	1.86	0.44–7.82	0.4			
Differentiation (mod)	2.06	0.98–4.33	0.052			
Depth (T3,T4)	3.6	0.86–15.1	0.08			
Lymphatic permeation	9.77	1.33–71.7	*0.025*	3.93	0.51–30.5	0.19
Venous permeation	2.21	0.85–5.78	0.1			
Lymph node metastasis	4.5	2.00–10.1	*0.0003*	2.01	0.86–4.67	0.11
Hematogenous metastasis	6.1	2.97–12.5	*<0.0001*	3.13	1.49–6.60	*0.0027*
CEACAM1-L dominance	7.72	2.34–25.5	*0.0008*	4.26	1.25–14.52	*0.02*

The italic fonts given for *p*-values of less than 0.05.
Abbreviations: Mod: moderately differentiated adenocarcinoma; CEACAM1-L dominance: CEACAM1-long isoform dominance; HR: hazard ratio; CI: confidential interval.

CEACAM1 long cytoplasmic domain isoform dominance and survival

To address that CEACAM1 cytoplasmic isoform balance is associated shorter survival of the patients with colorectal cancer, we performed statistical analyses regarding survival of colorectal cancer patients. The univariate analyses for survival are summarized in Table 3. Lymphatic permeation, lymph node metastasis, hematogenous metastasis and CEACAM1-L dominance were found to have prognostic value. A multivariate analysis with these four parameters, with significant prognostic values in the univariate analysis, revealed that hematogenous metastasis and CEACAM1-L dominance were independent prognostic factors (Table 3). The Kaplan–Meier method for the overall survival analysis showed that CEACAM1-L dominance was significantly associated with a shorter survival time. The 5-year survival of the CEACAM1-L dominant group was 71.2% in comparison to 95% in the other group ($p < 0.0001$; Fig. 2*c*, panel *a*′). The high expression of the CEACAM1 group showed a tendency toward poor survival in comparison to the low expression group, but there were no significant differences between the high expression group (77.2%) and the low expression group (86.8%, $p = 0.10$; Fig. 2*c*, panel *b*′). These results indicated that re-expression of CEACAM1 long cytoplasmic isoform at the invasion front of colorectal cancer is associated with survival of the patients with colorectal cancer.

The effect of CEACAM1 expression and cytoplasmic isoform balance on invasion and migration of colorectal cancer cell lines

Transfection of CEACAM1 shRNA into CEACAM1-overexpressing LS174T cells. To clarify that total CEACAM1 re-expression is important for colorectal cancer cell invasion and migration, and that knockdown of total CEACAM1 induced less invasive property of colorectal cancer cells, CEACAM1-overexpressing LS174T cells were transfected with shRNA targeted to CEACAM1. CEACAM1 shRNA plasmid led to less expression of total CEACAM1. Stable CEACAM1 shRNA significantly inhibited CEACAM1 protein expression levels compared to the vector control in Figure 3*a*. Invasion chamber experiments revealed that CEACAM1 shRNA suppressed invasion in Figure 3*b*. Wound healing assays also demonstrated that CEACAM1 shRNA exhibited lower levels of migration in Figure 3*c*. These results suggested that CEACAM1 re-expression plays an important role for invasion and migration of colorectal cancer cells.

Transfection of CEACAM1-4L or -4S into HT29 cells. To investigate that CEACAM1 cytoplasmic domain isoform balance

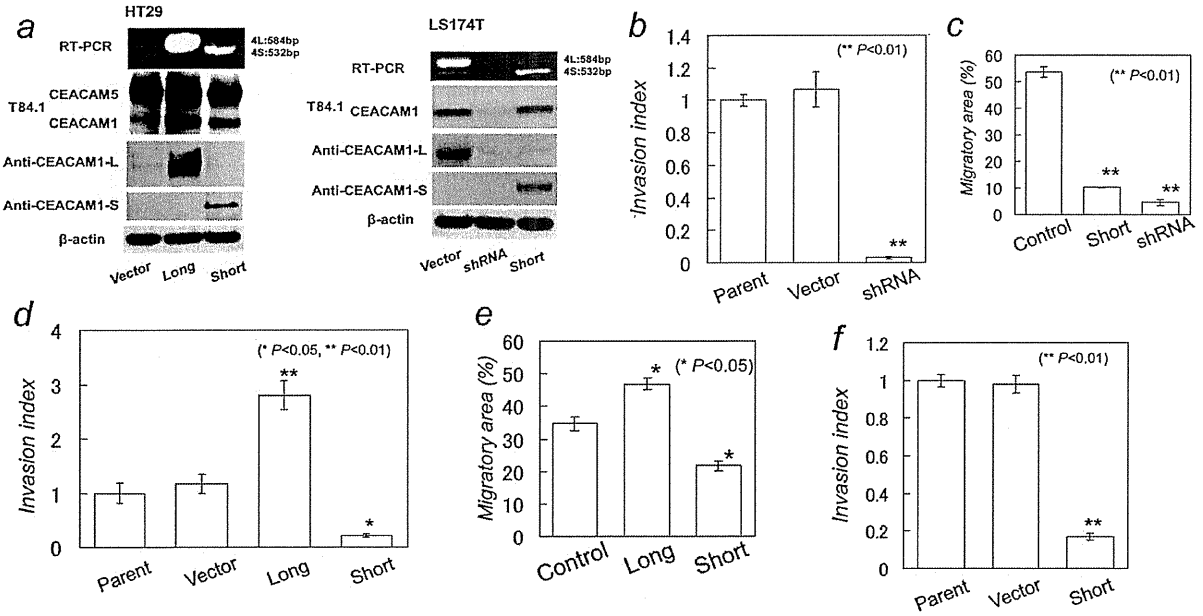

Figure 3. Transfection of CEACAM1-4L enhanced invasion and migration, and transfection of CEACAM1-4S or CEACAM1 knockdown reduced invasion and migration. (*a*) The Western blotting analyses and reverse transcriptase-polymerase chain reaction (RT-PCR). Left panel (HT29 cells); RT-PCR revealed that CEACAM1-L-transfected HT29 cells (Long) enhanced CEACAM1-L expression at mRNA level compared to empty vector-transfected HT29 (Vector). CEACAM1-S-transfected HT29 cells (Short) enhanced CEACAM1-S expression at mRNA level compared to empty vector-transfected HT29 (Vector). Stable CEACAM1-4L-transfected HT29 cells (Long) expressed significantly elevated CEACAM1-4L at protein level compared to vector-transfected cells (Vector). Stable CEACAM1-4S-transfected HT29 cells (Short) expressed significantly elevated CEACAM1-4S at protein level compared to vector-transfected cells (Vector). Right panel (LS174T cells); RT-PCR revealed that shRNA-transfected LS174T cells (shRNA) inhibited CEACAM1 expression at mRNA level compared to empty vector-transfected LS174T cells (Vector). CEACAM1-S-transfected LS174T cells (Short) enhanced CEACAM1-S expression at mRNA level compared to empty vector-transfected LS174T cells (Vector). Stable CEACAM1 shRNA-transfected LS174T cells (shRNA) significantly inhibited CEACAM1 protein expression levels compared to the vector control-transfected LS174T cells (Vector). Stable CEACAM1-4S-transfected LS174T cells (Short) expressed significantly elevated CEACAM1-4S at protein level compared to vector control-transfected LS174T cells (Vector). Anti-CEACAM1-L: CEACAM1 long cytoplasmic domain isoform specific rabbit polyclonal antibodies; anti-CEACAM1-S: CEACAM1 short cytoplasmic domain isoform specific mouse polyclonal antibodies. (*b*) Matrigel invasion assay. shRNA knockdown (CEACAM1 shRNA-transfected LS174T cells) was less invasive than parent (LS174T parent cells) or vector (vector control-transfected LS174T cells). (*c*) Wound healing assay. Both short (CEACAM1-4S-transfected LS174T cells) and shRNA (CEACAM1 shRNA-transfected LS174T cells) suppressed the migration. (*d*) Matrigel invasion assay. Long (CEACAM1-4L-transfected HT29 cells) exhibited increased invasion compared to parent (HT29 parent cells) or vector (vector control-transfected HT29 cells) samples. Conversely, short (CEACAM1-4S-transfected HT29 cells) significantly decreased invasion. (*e*) Wound healing assay. Long (CEACAM1-4L-transfected HT29 cells) showed more migration than control (vector control-transfected HT29 cells). Short (CEACAM1-4S-transfected HT29 cells) suppressed migration. (*f*) Matrigel invasion assay. Short (CEACAM1-4S-transfected LS174T cells) showed less invasion than parent (LS174T parent cells) or vector (vector control-transfected LS174T cells).

plays a crucial role for colorectal cancer invasion, we modulated CEACAM1 cytoplasmic domain isoform expression levels of HT29 colorectal cancer cells, hypoexpressing both CEACAM1-4L and -4S, by transfection with a plasmid encoding CEACAM1-4L or -4S. Stable CEACAM1-4L- or CEACAM1-4S-transfected HT29 cells expressed significantly elevated CEACAM1-4L and -4S at protein levels compared to vector-transfected cells in Figure 3*a*. The invasion chamber experiments revealed that CEACAM1-4L promoted invasion, and that CEACAM1-4S inhibited the invasion of HT29 cells in Figure 3*d*. Wound healing assays demonstrated that CEACAM1-4L promoted migration, and that CEACAM1-4S suppressed migration in Figure 3*e*. These results indicated that the status of CEACAM1 long cytoplasmic isoform dominance is important for colorectal cancer invasion and migration.

Transfection of CEACAM1-4S into CEACAM1-4L-overexpressing LS174T cells. To address the suppressive effect of CEACAM1-4S dominance on colorectal cancer invasion and migration, CEACAM1-4L-overexpressing LS174T cells transfected with a plasmid encoding CEACAM1-4S. Transfection of CEACAM1-4S induced CEACAM1 short cytoplasmic

domain isoform dominance. Stable CEACAM1-4S significantly inhibited CEACAM1 protein expression levels compared to the vector control in Figure 3*a*. Invasion chamber experiments revealed that CEACAM1-4S suppressed invasion in Figure 3*f*. Wound healing assays demonstrated that CEACAM1-4S exhibited lower levels of migration in Figure 3*c*. These results confirmed that CEACAM1 cytoplasmic domain isoform balance plays a crucial role for invasive and migrative properties in colorectal cancer cells.

Discussion

CEACAM1 is known to be downregulated at RNA level in adenoma[18] and carcinoma.[3] Some recent reports[9,10] have shown that CEACAM1 is overexpressed at protein level in colorectal cancer and correlated with clinical stage. The reason why colorectal cancer cells re-expressed CEACAM1 remains unclear. Our study clearly demonstrated that the expression of both CEACAM1-L and -S was weak at the luminal surface of advanced colorectal cancers, and that the expression of CEACAM1 was more intense at the invasion front of advanced colorectal cancers, suggesting that CEACAM1 long cytoplasmic domain isoform is associated with colorectal cancer invasion. Moreover, we showed that CEACAM1-L dominance, in comparison with CEACAM1-S, at the invasion front of colorectal cancer is associated with lymph node involvement, hematogenous metastasis and shorter survival of the patients, indicating that re-expression of CEACAM1, particular long cytoplasmic domain isoform, may function for invasion and migration of colorectal cancer.

To clarify that CEACAM1 re-expression induced invasion and migration, and that CEACAM1 cytoplasmic isoform balance was associated with colorectal cancer cells invasion and migration, we performed experiments of total CEACAM1 knockdown or of overexpression of two different cytoplasmic domain isoforms of CEACAM1. Strong invasiveness of LS174T cells was inhibited by downregulation of total CEACAM1 expression, suggesting that re-expression of total CEACAM1, which was observed at the invasion front of colorectal cancer tissues, promotes cancer cell invasion and migration. In terms of cytoplasmic isoform balance, overexpression of CEACAM1 long cytoplasmic domain isoform promoted invasiveness and motility of colorectal cancer cells, whereas short cytoplasmic domain isoform dominance by overexpression of CEACAM-4S decreased both HT29 and LS174T cellular invasion and migration. The finding that CEACAM1-4L promotes tumor cell invasion is consistent with other studies examining thyroid cancer[19] and malignant melanoma cells.[20] These data strengthened the view that re-expression of CEACAM1 and CEACAM1-L dominance is associated with invasion and metastasis in colorectal cancer.

The molecular mechanism of CEACAM1 on colorectal cancer invasion and migration remains to be elucidated. Some reports have shown the possible molecular mechanisms. A recombinant cytoplasmic domain of CEACAM1-L was specifically associated with the beta3 integrin subunit in neutrophils,[21] and beta3 integrin colocalized with CEACAM1 in melanoma.[20] The migratory effect of CEACAM1-L depends on integrins. CEACAM1-L and beta3 integrin were functionally interconnected with respect to invasive growth.[20] CEACAM1-L also enhanced cell–matrix adhesion and migration and promoted tumor invasiveness in thyroid cancer.[19] Our study found that cancer cell invasion and migration, lymph node involvement and hematogenous metastases were associated with CEACAM1-L dominance at the invasive front of colorectal cancers. Although further investigation is required for confirmation of the mechanism that CEACAM1 interacts with molecules that are involved in colorectal cancer invasion and migration, a similar mechanism such as the beta3 integrin and cell–matrix interaction with CEACAM1-L may occur in colorectal cancer invasion.

CEACAM1 cytoplasmic domain isoform balance is crucial for the function of CEACAM1. The balance of CEACAM1 isoforms expression was evaluated in epithelial cells.[22–24] Two CEACAM1 isoforms normally coexist in many normal tissues, with the longer isoform usually present in lower amounts than the shorter form.[23] CEACAM1-L accounts for 15–20% of total CEACAM1 expressed in normal colonic epithelial cells.[23] The CEACAM1-L isoform exhibits a tumor inhibition phenotype when expressed at physiological concentrations and in the appropriate ratio relative to the CEACAM1-S isoform. However, a significant overexpression of the CEACAM1-L isoform or a disruption of the normal ratio of L and S tail CEACAM1 expression abrogated tumor inhibition.[23] Therefore, an evaluation of the relative ratio of the CEACAM1 isoforms represents the characteristics of the cancer more accurately than the intensity of CEACAM1-L and -S expression. Our study also showed that the intensity of CEACAM1-L and -S expression did not significantly reflect the survival time of the patients with colorectal cancer. This result is consistent with the finding that the CEACAM1 expression is not significantly related to survival in colorectal cancer.[9] Therefore, an analysis of the relative expression levels of cytoplasmic domain isoform is required for evaluating the role of CEACAM1.

Our study demonstrated that CEACAM1-L isoform dominance is an independent risk factor for lymph node metastasis and hematogenous metastasis and is also an independent prognostic factor for overall survival. The overall survival analysis revealed that CEACAM1-L dominance was significantly associated with a shorter survival. The 5-year survival rate of the CEACAM1-L dominant group was 71.2% in comparison to 95% for the other group, indicating that the balance of CEACAM1-L and -S isoform expression in a tumor predicts the risk for lymph node and hematogenous metastasis and also predicts a poor prognosis. This may allow the identification of patients at a high risk and who may require adjuvant therapy after surgical resection.

Our study showed that the manipulation of CEACAM1 cytoplasmic domain isoform balance can control cancer cell migration and invasion. CEACAM1 expression is

known to be induced by all-trans-retinoic acid (ATRA) and gamma interferon. Continuous ATRA treatment of a human leukemia cell line induced the expression of CEACAM1 and resulted in apoptosis.[25] Gamma interferon also induced CEACAM1 in a colon cancer cell line.[26–28] However, as both ATRA and gamma interferon induce not only CEACAM1-S but also total CEACAM1, further investigation is required to develop an isoform-specific inducer.

In conclusion, our study clearly demonstrated that re-expression of CEACAM1 was observed mainly at the invasion front of colorectal cancer. Long cytoplasmic domain isoform dominance is associated with metastasis and shorter survival of colorectal cancer. Overexpression of CEACAM1 long cytoplasmic domain isoform, not CEACAM1 short cytoplasmic domain isoform, promoted invasion and migration of colorectal cancer cells. The modulation of CEACAM1 cytoplasmic isoform balance, such as by CEACAM1-S overexpression, may be a novel strategy for anti-invasion therapy.

Acknowledgements

The writing assistance was provided by Dr. Brian Quinn, Editor-in-Chief, Japan Medical Communication.

References

1. Thompson JA, Grunert F, Zimmermann W. Carcinoembryonic antigen gene family: molecular biology and clinical perspectives. *J Clin Lab Anal* 1991;5:344–66.
2. Nittka S, Gunther J, Ebisch C, Erbersdobler A, Neumaier M. The human tumor suppressor CEACAM1 modulates apoptosis and is implicated in early colorectal tumorigenesis. *Oncogene* 2004; 23:9306–13.
3. Neumaier M, Paululat S, Chan A, Matthaes P, Wagener C. Biliary glycoprotein, a potential human cell adhesion molecule, is down-regulated in colorectal carcinomas. *Proc Natl Acad Sci USA* 1993;90:10744–8.
4. Riethdorf L, Lisboa BW, Henkel U, Naumann M, Wagener C, Loning T. Differential expression of CD66a (BGP), a cell adhesion molecule of the carcinoembryonic antigen family, in benign, premalignant, and malignant lesions of the human mammary gland. *J Histochem Cytochem* 1997;45:957–63.
5. Luo W, Tapolsky M, Earley K, Wood CG, Wilson DR, Logothetis CJ, Lin SH. Tumor-suppressive activity of CD66a in prostate cancer. *Cancer Gene Ther* 1999;6:313–21.
6. Bamberger AM, Riethdorf L, Nollau P, Naumann M, Erdmann I, Gotze J, Brummer J, Schulte HM, Wagener C, Loning T. Dysregulated expression of CD66a (BGP, C-CAM), an adhesion molecule of the CEA family, in endometrial cancer. *Am J Pathol* 1998;152: 1401–6.
7. Thies A, Moll I, Berger J, Wagener C, Brummer J, Schulze HJ, Brunner G, Schumacher U. CEACAM1 expression in cutaneous malignant melanoma predicts the development of metastatic disease. *J Clin Oncol* 2002;20:2530–6.
8. Laack E, Nikbakht H, Peters A, Kugler C, Jasiewicz Y, Edler L, Brummer J, Schumacher U, Hossfeld DK. Expression of CEACAM1 in adenocarcinoma of the lung: a factor of independent prognostic significance. *J Clin Oncol* 2002;20: 4279–84.
9. Jantscheff P, Terracciano L, Lowy A, Glatz-Krieger K, Grunert F, Micheel B, Brummer J, Laffer U, Metzger U, Herrmann R, Rochlitz C. Expression of CEACAM6 in resectable colorectal cancer: a factor of independent prognostic significance. *J Clin Oncol* 2003;21:3638–46.
10. Kang WY, Chen WT, Wu MT, Chai CY. The expression of CD66a and possible roles in colorectal adenoma and adenocarcinoma. *Int J Colorectal Dis* 2007; 22:869–74.
11. Barnett TR, Drake L, Pickle W, II. Human biliary glycoprotein gene: characterization of a family of novel alternatively spliced RNAs and their expressed proteins. *Mol Cell Biol* 1993;13:1273–82.
12. Brummer J, Neumaier M, Gopfert C, Wagener C. Association of pp60c-src with biliary glycoprotein (CD66a), an adhesion molecule of the carcinoembryonic antigen family downregulated in colorectal carcinomas. *Oncogene* 1995;11:1649–55.
13. Huber M, Izzi L, Grondin P, Houde C, Kunath T, Veillette A, Beauchemin N. The carboxyl-terminal region of biliary glycoprotein controls its tyrosine phosphorylation and association with protein-tyrosine phosphatases SHP-1 and SHP-2 in epithelial cells. *J Biol Chem* 1999; 274:335–44.
14. Schumann D, Chen CJ, Kaplan B, Shively JE. Carcinoembryonic antigen cell adhesion molecule 1 directly associates with cytoskeleton proteins actin and tropomyosin. *J Biol Chem* 2001;276: 47421–33.
15. Gunning P, Leavitt J, Muscat G, Ng SY, Kedes L. A human beta-actin expression vector system directs high-level accumulation of antisense transcripts. *Proc Natl Acad Sci USA* 1987;84:4831–5.
16. Hinoda Y, Neumaier M, Hefta SA, Drzeniek Z, Wagener C, Shively L, Hefta LJ, Shively JE, Paxton RJ. Molecular cloning of a cDNA coding biliary glycoprotein I: primary structure of a glycoprotein immunologically crossreactive with carcinoembryonic antigen. *Proc Natl Acad Sci USA* 1988;85:6959–63.
17. Barnett TR, Kretschmer A, Austen DA, Goebel SJ, Hart JT, Elting JJ, Kamarck ME. Carcinoembryonic antigens: alternative splicing accounts for the multiple mRNAs that code for novel members of the carcinoembryonic antigen family. *J Cell Biol* 1989;108:267–76.
18. Nollau P, Scheller H, Kona-Horstmann M, Rohde S, Hagenmuller F, Wagener C, Neumaier M. Expression of CD66a (human C-CAM) and other members of the carcinoembryonic antigen gene family of adhesion molecules in human colorectal adenomas. *Cancer Res* 1997;57: 2354–7.
19. Liu W, Wei W, Winer D, Bamberger AM, Bamberger C, Wagener C, Ezzat S, Asa SL. CEACAM1 impedes thyroid cancer growth but promotes invasiveness: a putative mechanism for early metastases. *Oncogene* 2007;26:2747–58.
20. Ebrahimnejad A, Streichert T, Nollau P, Horst AK, Wagener C, Bamberger AM, Brummer J. CEACAM1 enhances invasion and migration of melanocytic and melanoma cells. *Am J Pathol* 2004;165: 1781–7.
21. Brummer J, Ebrahimnejad A, Flayeh R, Schumacher U, Loning T, Bamberger AM, Wagener C. cis Interaction of the cell adhesion molecule CEACAM1 with integrin beta(3). *Am J Pathol* 2001;159: 537–46.
22. Sundberg U, Obrink B. CEACAM1 isoforms with different cytoplasmic domains show different localization, organization and adhesive properties in polarized epithelial cells. *J Cell Sci* 2002; 115:1273–84.
23. Turbide C, Kunath T, Daniels E, Beauchemin N. Optimal ratios of biliary glycoprotein isoforms required for inhibition of colonic tumor cell growth. *Cancer Res* 1997;57:2781–8.
24. Sundberg U, Beauchemin N, Obrink B. The cytoplasmic domain of CEACAM1-L

controls its lateral localization and the organization of desmosomes in polarized epithelial cells. *J Cell Sci* 2004;117: 1091–104.

25. Ozeki M, Shively JE. Differential cell fates induced by all-trans retinoic acid-treated HL-60 human leukemia cells. *J Leukoc Biol* 2008;84:769–79.
26. Takahashi H, Okai Y, Paxton RJ, Hefta LJ, Shively JE. Differential regulation of carcinoembryonic antigen and biliary glycoprotein by gamma-interferon. *Cancer Res* 1993;53:1612–19.
27. Chen CJ, Lin TT, Shively JE. Role of interferon regulatory factor-1 in the induction of biliary glycoprotein (cell CAM-1) by interferon-gamma. *J Biol Chem* 1996;271:28181–8.
28. Chen CJ, Li LJ, Maruya A, Shively JE. In vitro and in vivo footprint analysis of the promoter of carcinoembryonic antigen in colon carcinoma cells: effects of interferon gamma treatment. *Cancer Res* 1995;55: 3873–82.

Tumor-infiltrating CD4+ Th17 cells produce IL-17 in tumor microenvironment and promote tumor progression in human gastric cancer

TAKESHI IIDA[1], MAKOTO IWAHASHI[1], MASAHIRO KATSUDA[1], KOICHIRO ISHIDA[1], MIKIHITO NAKAMORI[1], MASAKI NAKAMURA[1], TEIJI NAKA[1], TOSHIYASU OJIMA[1], KENTARO UEDA[1], KEIJI HAYATA[1], YASUSHI NAKAMURA[2] and HIROKI YAMAUE[1]

[1]Second Department of Surgery, [2]Division of Pathology, Department of Clinical Laboratory Medicine, School of Medicine, Wakayama Medical University, Wakayama 641-8510, Japan

Received December 2, 2010; Accepted January 27, 2011

DOI: 10.3892/or.2011.1201

Abstract. Recently, a subset of IL-17 producing T cells distinct from Th1 or Th2 cells has been described as key players in inflammation and autoimmune diseases as well as cancer development. In this study, we investigated the expression level of IL-17 and T helper 17 (Th17)-related cytokines in gastric cancer tissues and assessed the association of their expression with angiogenesis and their clinicopathological parameters. Tumor and adjacent normal tissues were obtained from 82 patients with gastric cancer. IL-17, IL-21 and IL-23 mRNA expression levels were quantified by real-time RT-PCR. Th17 infiltration, microvessel density and neutrophil infiltration in tumor tissues were examined by immunohistochemistry and double immunofluorescence histochemistry. Expression of IL-17, IL-21 and IL-23 mRNA was found to be significantly up-regulated in tumor tissues compared with adjacent normal tissues. The expression level of IL-17 mRNA strongly and positively correlated with that of IL-21 mRNA in tumor tissue. The number of vascular endothelial cells and infiltrating neutrophils was significantly larger in tumors expressing a high level of IL-17 mRNA than in tumors expressing a low level of IL-17 mRNA. In tumor tissues most CD4+ cells were stained with anti-IL-17 antibody. The expression level of IL-17 mRNA in gastric tumors was associated with the depth of the tumors, lymph-vascular invasion and lymph node involvement, suggesting that IL-17 obviously was related to tumor progression. IL-17 and IL-21, which regulates IL-17, would be potential therapeutic targets for the treatment of gastric cancer.

Correspondence to: Dr Makoto Iwahashi, Second Department of Surgery, Wakayama Medical University, School of Medicine, 811-1 Kimiidera, Wakayama 641-8510, Japan
E-mail: makoto@wakayama-med.ac.jp

Key words: Th17, IL-17, IL-21, gastric cancer, angiogenesis, inflammation

Introduction

It has been established that cancer can be promoted or exacerbated by inflammation and infection. Chronic inflammation is a major driving force in tumor development (1-3). Interleukin (IL)-17 is considered a proinflammatory cytokine because it has been shown to increase the production of IL-6 and IL-8 in macrophages and fibroblasts (4-6). Recently a new lineage of effector CD4+ T cells characterized by production of IL-17, the T helper 17 (Th17) lineage, was described on the basis of developmental and functional features that are distinct from those of classic Th1 and Th2 lineages (7). The identification of this new subtype of Th17 cell has prompted renewed interest in IL-17 biology. IL-17 plays an important role in inflammation, and is critical in host defense against infectious disease, allergy, and autoimmune diseases such as rheumatoid arthritis and inflammatory bowel diseases, which include Crohn's disease and ulcerative colitis (8,9). Interestingly, IL-17 also has been reported to be up-regulated in *Helicobacter pylori* (Hp) infected gastric mucosa. IL-17 positively regulates the synthesis of IL-8 by gastric mononuclear cells and epithelial cells, which thus emphasizes the role of IL-17 in Hp-driven inflammation (10).

Recently, it has been reported that IL-17 promotes tumor growth through angiogenesis in mice (11). On the other hand, several reports have shown that IL-17 inhibits tumor growth through antitumor immunity in immunocompetent mice (12,13). It remains controversial whether IL-17 promotes or inhibits cancer progression. In humans, IL-17 expression has been reported in several tumor tissues such as ovarian cancer, colon cancer and also gastric cancer (14-16). Most solid tumors contain non-malignant cells, including immune cells and blood vessel cells, which are important in inflammation in the tumor microenvironment. In fact, a high percentage of CD4+ Th17 cells produce IL-17 at sites of ovarian cancer (17). However, in human tumors, the crucial molecular pathways that permit communication between abnormally growing cancer cells and these inflammatory cells remain unknown. In addition, the underlying mechanism of IL-17 at tumor sites in modulating tumor growth is still poorly understood.

Differentiation of Th17 cells from naïve T cells appears to involve signals from transforming growth factor β (TGF-β) and IL-6 (18,19). IL-21 has been reported to play an important role in the initial phase of Th17 differentiation (20,21). Although, in mice, there is a general agreement on the factors required for the generation of Th17 cells as mentioned above, the crucial initiating cytokines in humans for Th17 development remain unclear, and the relationship between IL-21 and IL-17 at tumor sites has not been elucidated.

In this study, we quantitatively investigated expression of IL-17 and IL-21 messenger RNA (mRNA) in gastric cancer tissues. In addition, we assessed the association of IL-17 expression levels with angiogenesis and neutrophil infiltration and its clinicopathological factors to clarify the role of tumor-infiltrating Th17 in tumor growth and progression. We also reviewed the possibility of IL-17 as a therapeutic target for patients with gastric cancer.

Materials and methods

Patients and tissue specimens. Included in the present study was a series of 82 patients (58 men, 24 women) with gastric cancer who underwent gastrectomy at Wakayama Medical University Hospital (WMUH) from 2004 to 2007. None of them received anticancer therapy before surgery. Individuals with concurrence of autoimmune disease, inflammatory bowel disease or viral infection were excluded. Clinicopathological characteristics of these 82 patients are summarized in Table I. Clinical stages of the tumors were determined according to the International Union Against Cancer TNM classification for gastric cancer. Samples of cancer tissues and non-cancerous adjacent tissues were collected from resected specimens of patients. Tumor samples were obtained from the invasive front of resected gastric cancer. Written informed consent was obtained from all patients before their participation in this study. In addition, the local ethics committee of WMUH approved this study.

RNA extraction and DNA synthesis. Total RNA was extracted with an RNeasy mini kit (Qiagen, Hilden, Germany) followed by RNase-Free DNase Set treatment (Qiagen). Complementary DNA was synthesized from 1 μg of total RNA by using the Reverse Transcription System (Promega) according to manufacturer's instructions.

Quantitative real-time RT-PCR. Quantitative real-time reverse transcription-polymerase chain reaction (RT-PCR) was performed with isolated total RNA (1 μg) on the LightCycler system (Roche Molecular Biochemicals, Mannheim, Germany). The following oligonucleotide primers and hybridization probes were used: human IL-17 sense, 5'-CTGGGAAGACC TCATTGG-3' and antisense, 5'-CCTTTTGGGATTGGTA TTGG-3', fluorescein-labeled probe, 5'-TCCTCAGAATTT GGGCATCCTGGATTTC-3', and LC Red 640-labeled probe, 5'-TGGGATTGTGATTCCTGCCTTCACTATGG-3'; human IL-21 sense, 5'-AGGTCAAGATCGCCACAT-3' and antisense, 5'-TTTGCTGACTTTAGTTGGGC-3', fluorescein-labeled probe, 5'-CTGACCACTCACAGTTTGTCTCTACATCTTCTG GA-3', and LC Red 640-labeled probe, 5'-CTGGCAGAAA TTCAGGGACCAAGTCATTCA-3'; human IL-23 sense, 5'-GAGAAGCTGCTAGGATCG-3', and antisense, 5'-TGG TGACCCTCAGGCTGC-3', fluorescein-labeled probe, 5'-GCC TTCTCTGCTCCCTGATAGCCCTGTG-3', and LC Red 640-labeled probe, 5'-GCCAGCTTCATGCCTCCCTACTG GG-3'; human glyceraldehyde 3-phosphate dehydrogenase (GAPDH) sense, 5'-TGAACGGGAAGCTCACTGG-3' and antisense, 5'-TCCACCACCCTGTTGCTGTA-3', fluorescein-labeled probe, 5'-TCAACAGCGACACCCACTCCT-3', and LC Red 640-labeled probe, 5'-CACCTTTGACGCTGGGGCT-3'. Primers and probes were designed by Nihon Gene Research

Table I. IL-17 mRNA expression and clinicopathological parameters.

Factor	No. of patients	Expression of IL-17 mRNA[a]	P-value
Gender			
Male	59	3.24±0.179	
Female	23	3.65±0.298	0.22
Age (years)			
<65	31	3.78±0.193	
≥65	51	3.11±0.212	0.118
Tumor stage[b]			
T0/T1	15	2.52±0.430	
T2	33	3.13±0.219	
T3	34	3.99±0.186	<0.005[a]
Histological type			
Differentiated	40	3.19±0.247	
Undifferentiated	42	3.52±0.188	0.658
Lymphatic invasion			
Negative	27	2.78±0.303	
Positive	55	3.65±0.164	<0.05[d]
Venous invasion			
Negative	43	2.95±0.226	
Positive	39	3.82±0.184	<0.05[d]
Lymph node metastasis			
Negative	40	2.95±0.234	
Positive	42	3.75±0.186	<0.05[d]
Stage[b]			
0/I	31	2.66±0.254	
II	21	3.63±0.297	
III	19	3.84±0.240	
IV	11	4.00±0.378	<0.05[c]
Tumor size (cm)			
<5	46	3.13±0.202	
≥5	36	3.63±0.232	0.068

[a]Expression of mRNA for IL-17 were corrected with GAPDH housekeeping control amplifications. Values represent mean ± SEM. [b]Stage according to the TNM classification for gastric cancer (UICC). [c]P-value of Kruskal-Wallis test as appropriate. [d]P-value of Mann-Whitney test as appropriate.

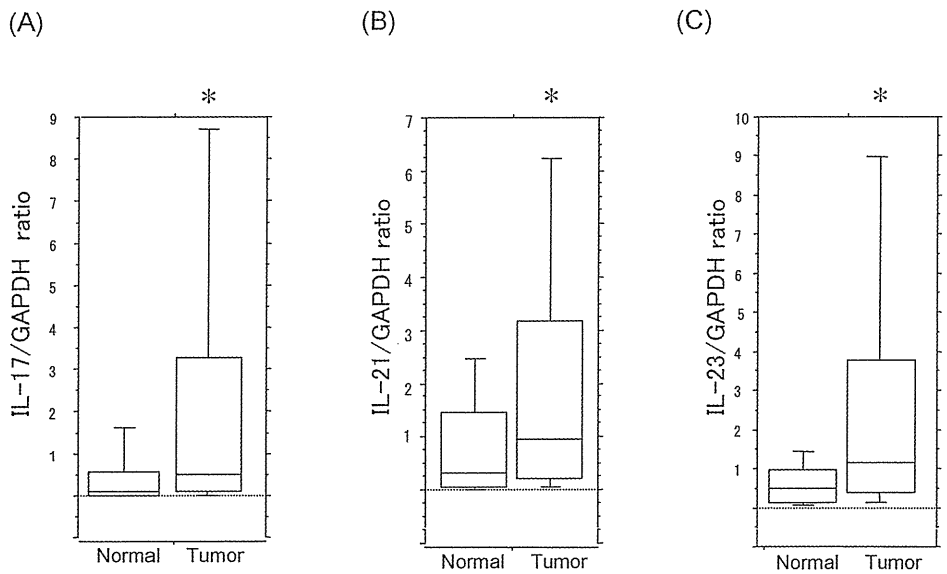

Figure 1. Level of IL-17, IL-21 and IL-23 mRNA expression in tumor and normal tissues of gastric cancer in 82 clinical samples. Expression levels of IL-17 (A), IL-21 (B) and IL-23 (C) mRNA were quantitatively determined by real-time RT-PCR for tumor tissue specimens and non-tumor tissue specimens from gastric cancer. Box plots show the 10th, 25th, 50th (median), 75th and 90th percentile values for log-transformed ratios of mRNA copies to GAPDH copies for IL-17, IL-21 and IL-23. *Significantly different from adjacent normal tissues ($p<0.0005$). Two-tailed p-values are based on the Mann-Whitney test.

Laboratories, Inc. (Miyagi, Japan). After 10 min of initial denaturation at 95°C, the cycling protocol entailed 40 cycles of denaturation at 95°C (10 sec), annealing at 62°C (15 sec) and elongation at 72°C (8 sec). For GAPDH, the thermocycling protocol was the same, except that annealing was performed at 55°C (15 sec) and 50 cycles were run. On each run, we quantified all samples according to the LightCycler software program, version 3.8 (Roche Molecular Biochemicals). The levels of mRNA for IL-17, IL-21 and IL-23 were corrected with GAPDH housekeeping control amplifications.

Immunohistochemistry and quantitative microscopy. Sections (4 μm) were prepared from paraffin-embedded blocks derived from gastric tumors. Sections were deparaffinized in xylene and graded alcohols, and rinsed in phosphate-buffered saline. Antigen retrieval from tissue was carried out by autoclaving the tissue in 0.01 M citrate buffer (pH 6.0) at 120°C for 10 min. The antibodies used included rabbit anti-IL-17 (dilution at 1:100, Santa Cruz Biotechnology); rabbit anti-IL-21 (dilution at 1:100, LifeSpan BioSciences); mouse anti-CD34, specific for endothelial tissue (dilution at 1:50, DakoCytomation, Glostrup, Denmark); and mouse anti-CD66b, specific for neutrophils (dilution at 1:500, BD Pharmingen). The antibodies were incubated overnight at 4°C. The immunocomplex was visualized by a polymer envision method, EnVision+ Kit (Dako). For quantification of tumor microvessel density and neutrophil infiltration, highly positive areas were initially identified by scanning tumor sections using light microscopy at low power. Areas of infarct-like necrosis and areas immediately adjacent to ulcerations were not considered in counts. Vessel counts were assessed according to the criteria of Weidner *et al* (22). Vessels in five high-power fields (x200 magnification) and neutrophil infiltration in five high-power fields (x400 magnification) were counted. Positive cells were quantified by an image processing application (Win ROOF, version 5.5; Mitani, Tokyo, Japan) and the manual counts were confirmed by a pathologist.

Double immunofluorescence histochemistry. Tissues were stained with primary antibodies: mouse anti-CD4 (dilution at 1:100, Dako) and rabbit anti-IL-17 (dilution at 1:100, Santa Cruz). The CD4 and IL-17 antibodies were detected with Alexa Fluor 488 conjugated goat anti-mouse immunoglobulin G (IgG) (Molecular Probes) and Alexa Fluor 546 conjugated goat anti-rabbit IgG (Molecular Probes). The double-stained sections were analyzed with a confocal laser scanning microscope (LSM5Pascal Exciter, version 4.0; Carl Zeiss, Jena, Germany).

Statistical analysis. The following statistical analyses were used. For data in Figs. 1, 3 and 4, we used the Mann-Whitney test. In Fig. 2, we used the Spearman rank correlation coefficient. In Table I, we used the Mann-Whitney test and the Kruskal-Wallis test. All statistical analyses were performed with StatView 6.0 (SAS Institute Inc) statistical software program. A value of $p<0.05$ was considered statistically significant.

Results

Expression of IL-17, IL-21 and IL-23 mRNA in tumor and non-cancerous tissues. IL-17 was found to be significantly up-regulated in tumor tissue compared with adjacent normal tissue ($p<0.0005$, Fig. 1A). Both IL-21 and IL-23, which are related to IL-17 production, were also significantly up-regulated in tumor tissue ($p<0.0005$, Fig. 1B and C).

Correlation of IL-17 mRNA with IL-21 and IL-23 mRNA in tumor tissues. The expression level of IL-17 mRNA positively correlated with that of IL-21 mRNA in tumor tissues ($r=0.730$,

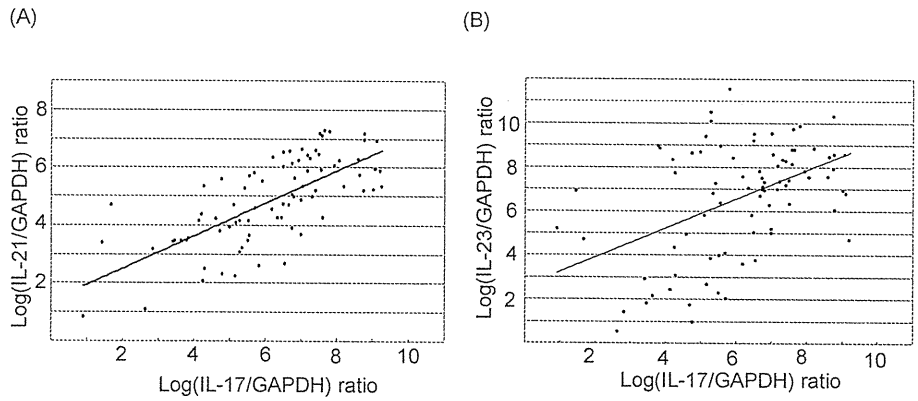

Figure 2. The correlation between expression levels of IL-17 mRNA, IL-21 mRNA and IL-23 mRNA. The correlation between expression levels of IL-17 mRNA and IL-21 mRNA [(A) r=0.730, p<0.0001], and the correlation between expression levels of IL-17 mRNA and IL-23 mRNA [(B) r=0.415, p<0.0005] were examined in tumor tissues. Log-transformed mRNA levels, normalized for GAPDH mRNA, are shown. The relationships are shown along with Spearman's rank-order correlation.

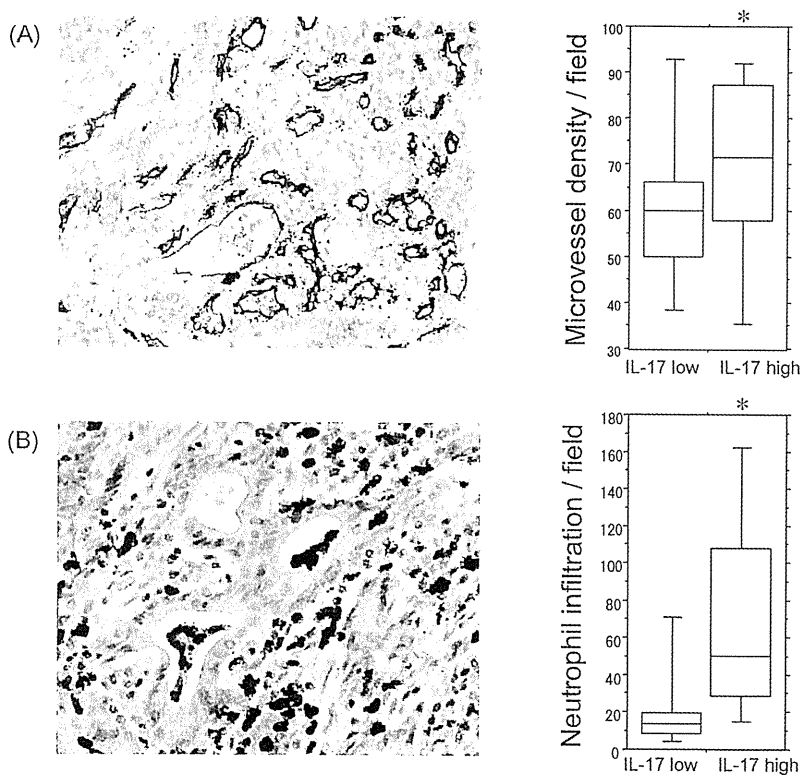

Figure 3. Microvessel density and neutrophils infiltration in tumor tissues. (A) Immunohistochemical staining of tumor tissues with anti-CD34 antibody, specific for endothelial tissues, was performed. Representative pictures of immunohistochemical staining of tumor tissues are shown. Vessels in five power fields (x200 magnification) were counted. (B) Immunohistochemical staining of tumor tissues with anti-CD66b antibody, specific for neutrophils, was performed. Representative pictures of immunohistochemical staining of tumor tissues are shown. Positive cells in five power fields (x400 magnification) were counted. Box plots show the 10th, 25th, 50th (median), 75th and 90th percentile values for the average number. *Significantly different from tumors expressing low levels of IL-17 (p<0.01). Two-tailed p-values are based on the Mann-Whitney test.

p<0.0001, Fig. 2A). On the other hand, there was no correlation between expression levels of IL-17 mRNA and IL-23 mRNA in tumor tissues (r=0.415, p<0.0005, Fig. 2B).

Quantification of tumor microvessel density. To assess the association between microvessel density and IL-17 expression in tumor tissue, we performed immunohistochemical staining with anti-CD34 antibody specific for endothelial cells. High- and low-expression groups were defined by the median value of IL-17 mRNA expression of this study population. The number of vascular endothelial cells was significantly higher in tumors expressing high IL-17 mRNA than in tumors expressing low IL-17 mRNA (p<0.01, Fig. 3A).

Quantification of tumor-infiltrating neutrophils. To assess the association between neutrophil infiltration and IL-17 expres-

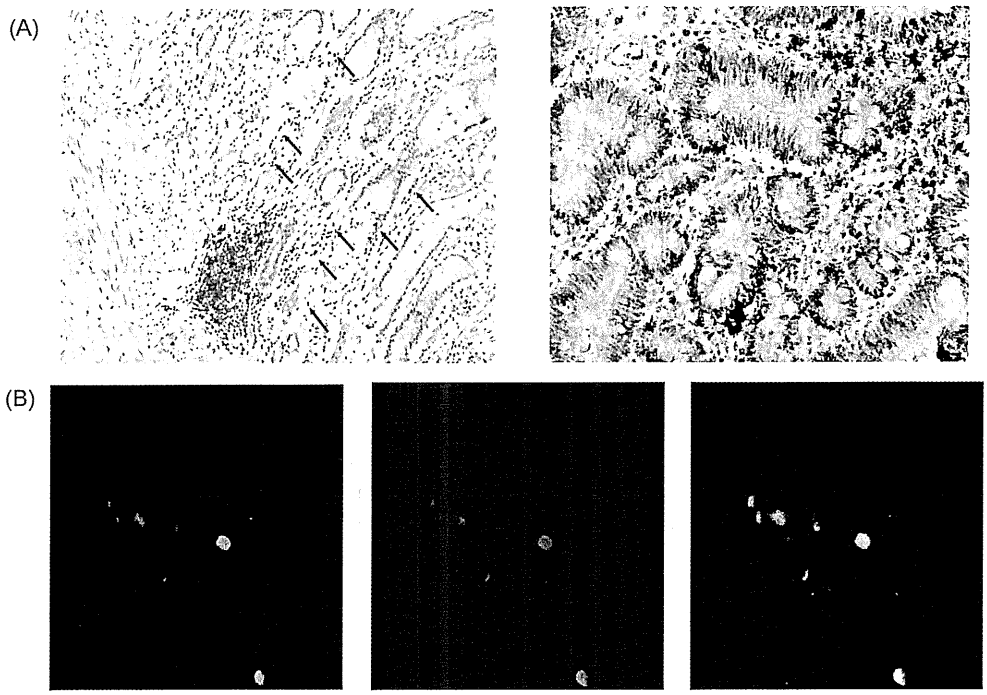

Figure 4. Immunohistochemistry for IL-17 in normal and tumor site. (A) Representative pictures of immunohistochemical staining with anti-IL-17 antibody at the normal (left panel) and tumor (right panel) site of gastric cancer specimens. More IL-17-positive cells were observed in the tumor tissues than in the adjacent normal tissues. The original magnification is x400. (B) Double immunofluorescence histochemistry for CD4 and IL-17 in tumor site. Tissue sections from a tumor were incubated with mouse monoclonal antibody against CD4 together with rabbit polyclonal antibodies against IL-17. The monoclonal antibody was detected with Alexa Fluor 488 conjugated goat anti-mouse IgG (green fluorescence; left panel), and the polyclonal antibodies were detected with Alexa Fluor 546 conjugated goat anti-rabbit IgG (red fluorescence; middle panel). Merged image of the two fluorophores is displayed in yellow (right panel). The original magnificationis x1000.

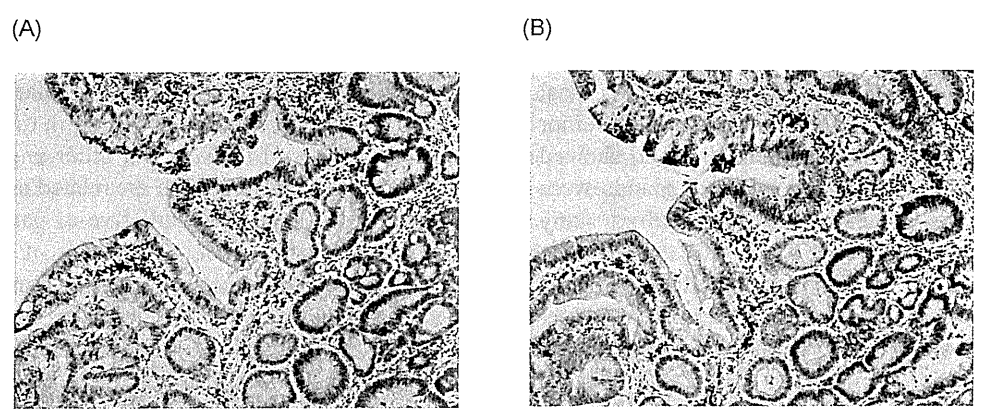

Figure 5. Immunohistochemistry for IL-17 and IL-21 in tumor site. (A) Representative pictures of immunohistochemical staining with anti-IL-17 antibody at the tumor site of gastric cancer specimens. (B) Representative pictures of immunohistochemical staining with anti-IL-21 antibody at the tumor site of gastric cancer specimens. The IL-21-positive cells did not always coincide with the IL-17-positive cells in the two serial sections. Original magnification x100.

sion in tumor tissue, we performed immunohistochemical staining with anti-CD66b antibody specific for neutrophils. High- and low-expression groups were defined by the median value of IL-17 mRNA expression of this study population. The number of infiltrating neutrophils was significantly lager in tumors expressing high IL-17 mRNA than in tumors expressing low IL-17 mRNA ($p<0.001$, Fig. 3B).

Distributions of IL-17-positive cells. To examine the expression of IL-17 in tumor and normal tissue, we performed immunohistochemistry for IL-17. IL-17 immunoreactive cells were rarely detected in non-cancerous adjacent tissues. On the other hand, there were abundant IL-17-expressing cells in tumor tissues; however, none of the tumor cells stained for IL-17 (Fig. 4A).

Identification of IL-17-producing cells in tumors. To identify IL-17-producing cells in tumor tissues, we performed double immunofluorescence histochemistry with anti-IL-17 and anti-CD4 antibodies in tumor tissues. The anti-CD4 primary